X-ray radiography of granular systems – particle densities and dynamics

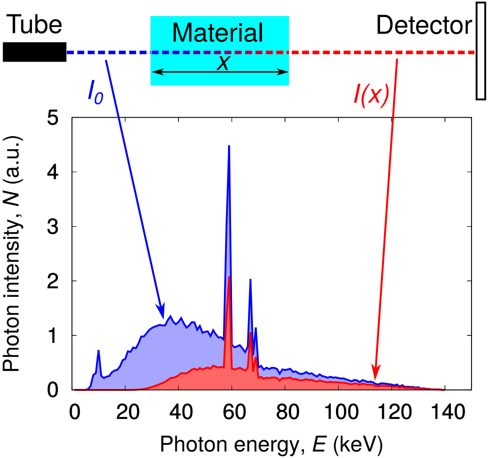

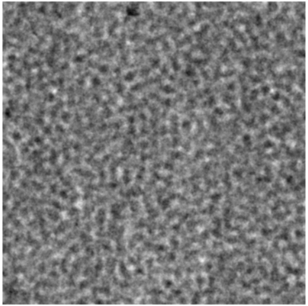

FRIEDRICH-ALEXANDER UNIVERSITÄT ERLANGEN-NÜRNBERG

Institute for Multiscale Simulation MSS

PhD defense

Manuel Baur

Funded by the German Federal Ministry for Economic Affairs and Energy, grant no. 50WM 1653

X-ray radiography of granular systems – particle densities and dynamics

X-ray radiography of granular systems – particle densities and dynamics

⋮

Granular materials are athermal

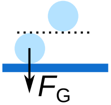

$$E_{pot} \approx 10^{10} E_{thermal}$$

X-ray radiography of granular systems – particle densities and dynamics

⋮

Granular materials are athermal

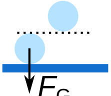

$$E_{pot} \approx 10^{10} E_{thermal}$$

Volume fraction

$$\Phi = \frac{V_{Particles}}{V_{Container}}$$

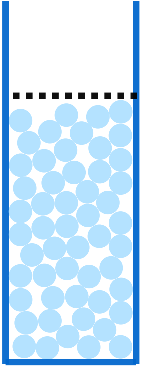

$$\Phi = \Phi_{RLP}$$

X-ray radiography of granular systems – particle densities and dynamics

⋮

Granular materials are athermal

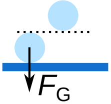

$$E_{\mathrm{pot}} \approx 10^{10} E_{\mathrm{thermal}}$$

Dissipative interactions

Driscoll *et al* (2016)

Volume fraction

$$\Phi = \frac{V_{\mathrm{Particles}}}{V_{\mathrm{Container}}}$$

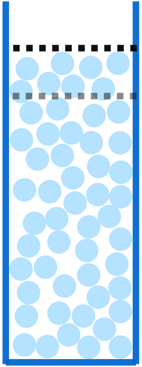

$$\Phi < \Phi_{\mathrm{RLP}}$$

$$\Phi = \Phi_{\mathrm{RLP}}$$

X-ray radiography of granular systems – particle densities and dynamics

⋮

Granular materials are athermal

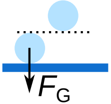

$$E_{pot} \approx 10^{10} E_{thermal}$$

Dissipative interactions

Driscoll *et al* (2016)

Volume fraction

$$\Phi = \frac{V_{Particles}}{V_{Container}}$$

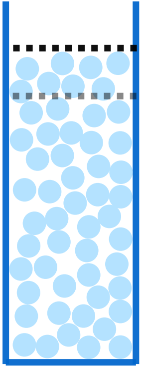

$\Phi < \Phi_{RLP}$

$\Phi = \Phi_{RLP}$

X-ray radiography of granular systems – particle densities and dynamics

Liquid fluidized bed

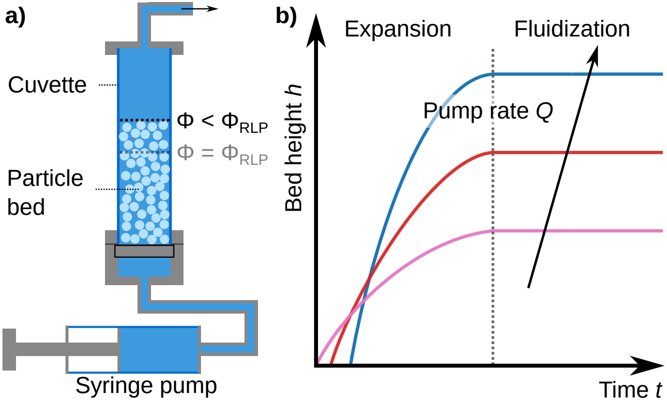

X-ray radiography of granular systems – particle densities and dynamics

Liquid fluidized bed

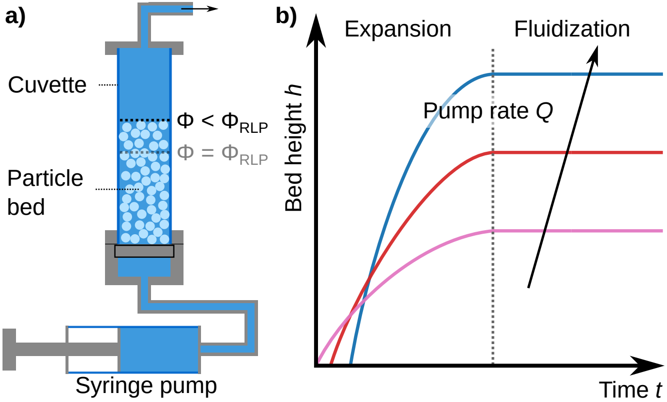

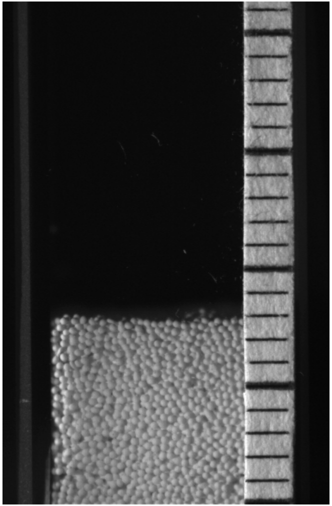

Master thesis Welm Pätzold

Particulate flows are **opaque**

X-ray radiography & tomography

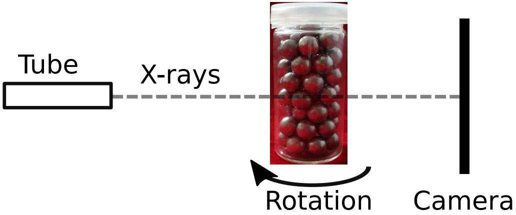

Radiogram

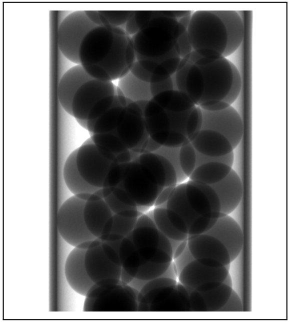

2D projections of 3D object

Short acquisition time

→ Dynamic system

X-ray radiography & tomography

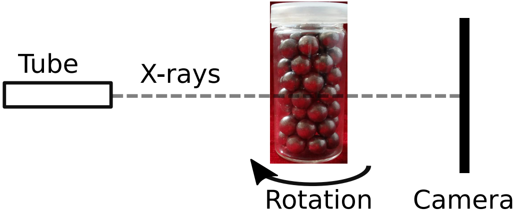

Radiogram

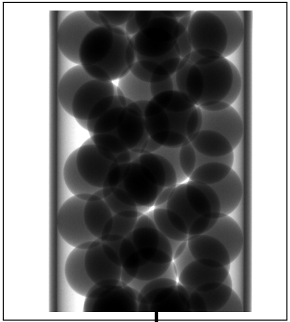

2D projections of 3D object
Short acquisition time
→ Dynamic system

Reconstruction from
800 projections

Tomogram

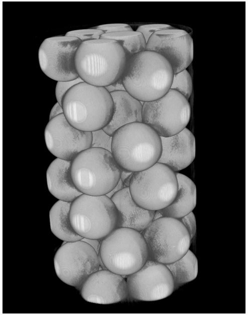

Full 3D information
Long acquisition time
→ Static objects

Measuring the volume fraction of **dynamic** granular systems

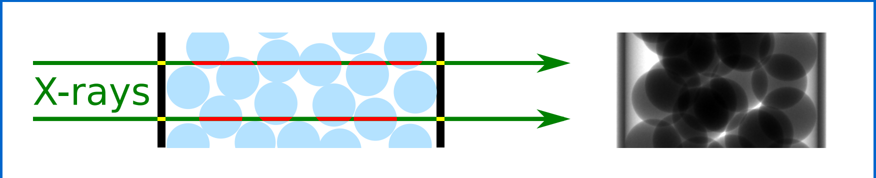

Correction of beam hardening in X-ray radiograms

Baur *et al*, *Rev. Sci. Instrum.* (2019)

In collaboration with Norman Uhlmann, Fraunhofer EZRT

Attenuation of X-rays

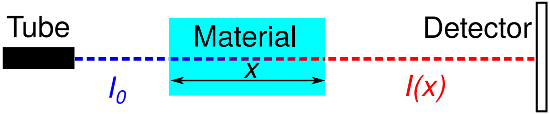

Beer-Lambert's law

$$I(x) = I_0 \exp(-\mu\, x)$$

Attenuation of X-rays

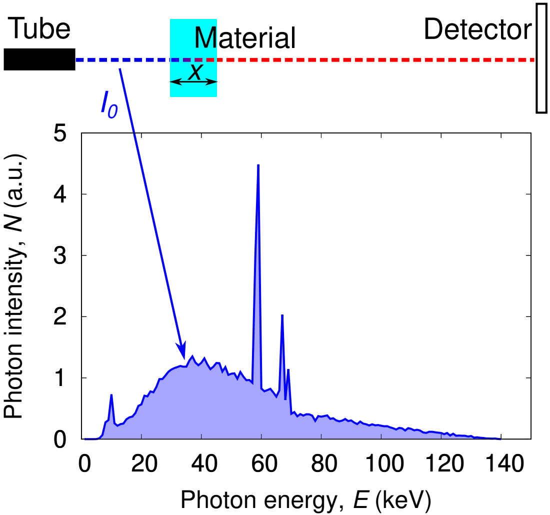

Beer-Lambert's law

$$I(x) = I_0 \exp(-\mu\, x)$$

Attenuation of X-rays

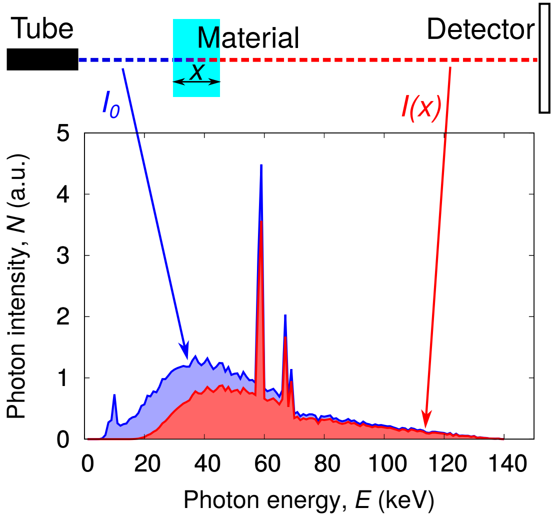

Beer-Lambert's law

$$I(x) = I_0 \exp(-\mu\, x)$$

Attenuation of X-rays

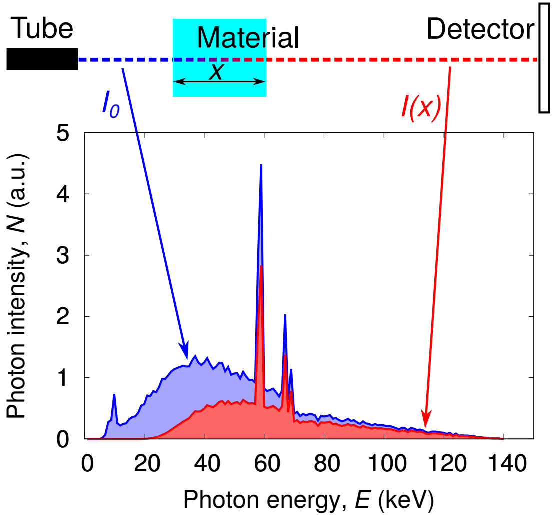

Beer-Lambert's law

$$I(x) = I_0 \exp(-\mu\, x)$$

Attenuation of X-rays

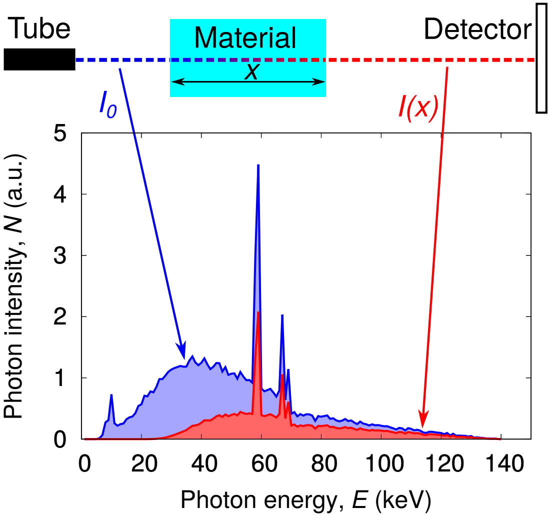

Beer-Lambert's law

$$I(x) = I_0 \exp(-\mu x)$$

Attenuation of X-rays

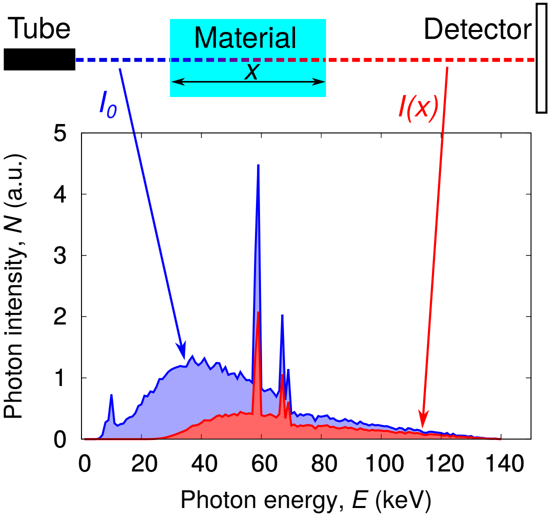

Beer-Lambert's law

$$\cancel{I(x) = I_0 \exp(-\mu\, x)}$$

$$I(x) = I_0 \exp(-\mu_{\text{eff}}(x)\, x)$$

Attenuation of X-rays

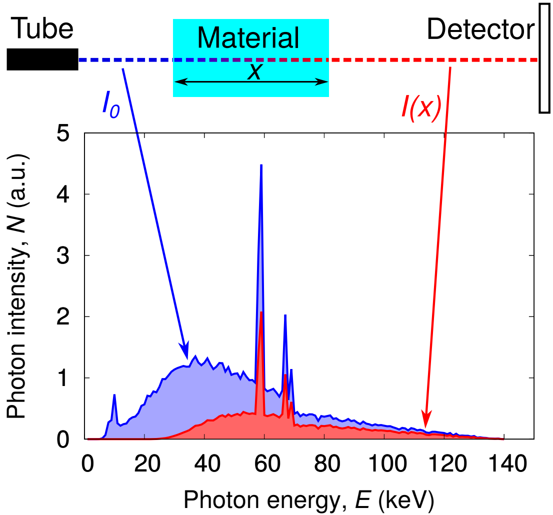

Beer-Lambert's law

$$\cancel{I(x) = I_0 \exp(-\mu\, x)}$$

$$I(x) = I_0 \exp(-\mu_{\text{eff}}(x)\, x)$$

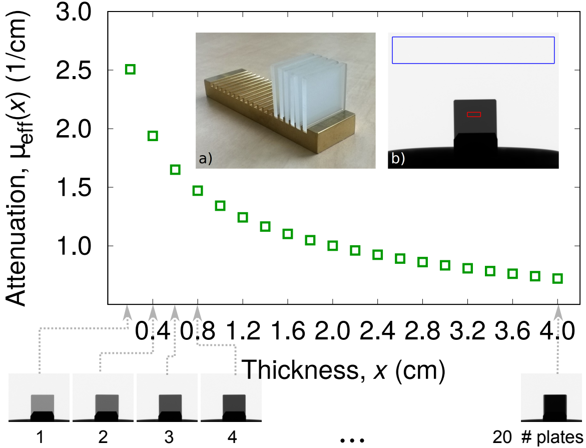

Attenuation of X-rays

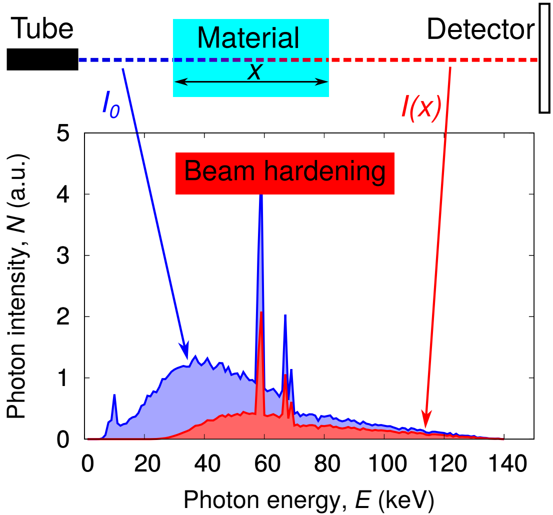

Beer-Lambert's law

$$I(x) = I_0 \exp(-\mu(E, Z, \rho)\, x)$$

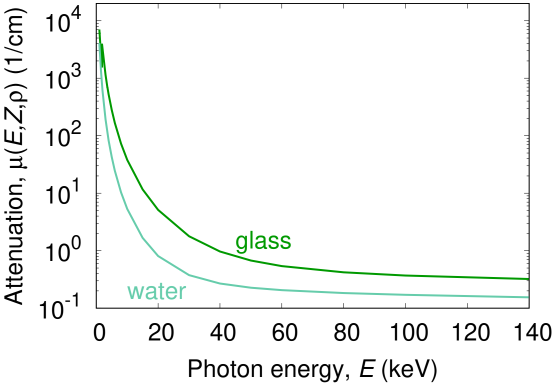

Tabulated attenuation coefficients from NIST.gov

Modeling of $\mu_{\text{eff}}(x)$

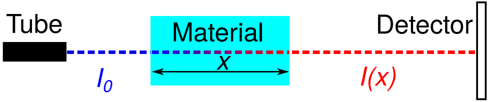

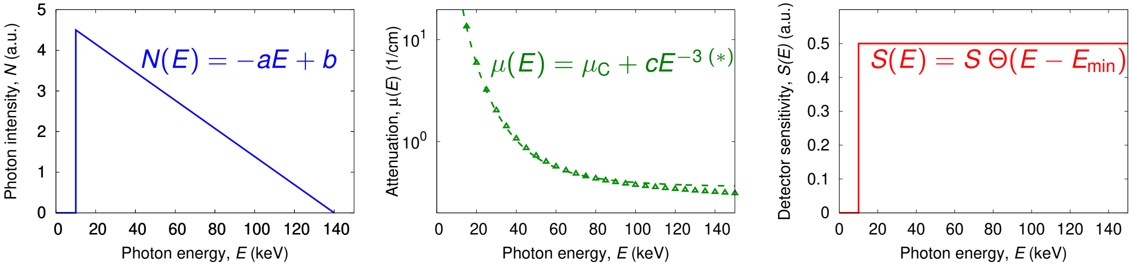

$$I(x) \propto \int N(E) \exp\{-\mu(E)x\} S(E)\, \mathrm{d}E$$

(∗) XCOM supplied by NIST

Modeling of $\mu_{\text{eff}}(x)$

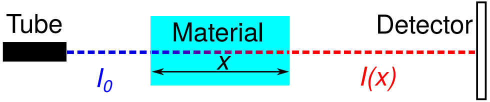

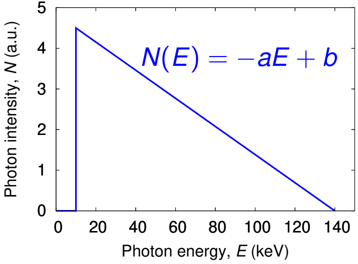

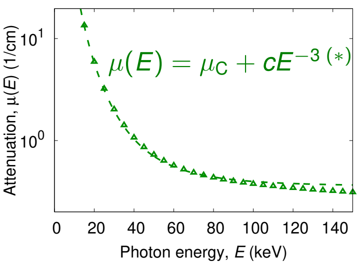

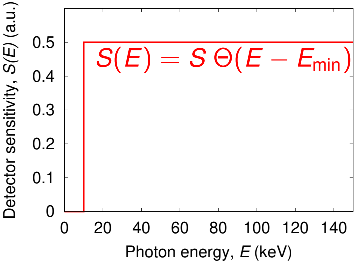

$$I(x) \propto \int N(E) \exp\{-\mu(E)x\} S(E)\, \mathrm{d}E$$

$$\propto S \int_{E_{\text{min}}}^{E_{\text{max}}} (-aE + b) \exp\{-(\mu_C + cE^{-3})x\}\, \mathrm{d}E$$

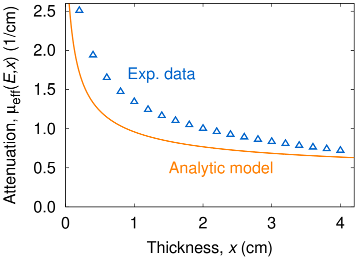

(∗) XCOM supplied by NIST

Modeling of $\mu_{\mathrm{eff}}(x)$

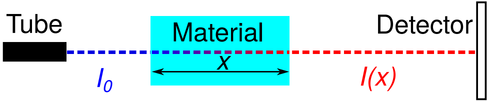

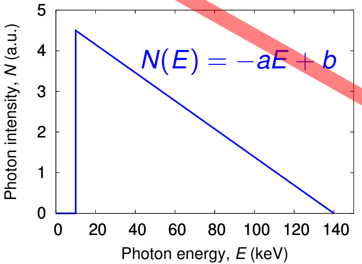

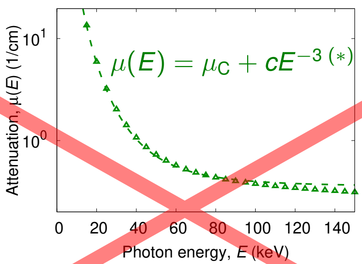

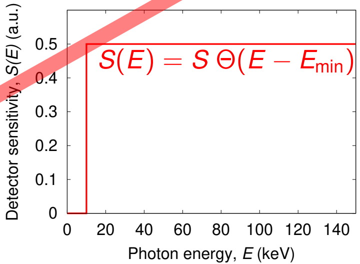

$$I(x) \propto \int N(E)\,\exp\{-\mu(E)x\}\,S(E)\,\mathrm{d}E$$

$$\propto S\int_{E_{\mathrm{min}}}^{E_{\mathrm{max}}}(-aE+b)\,\exp\{-(\mu_C+cE^{-3})x\}\,\mathrm{d}E$$

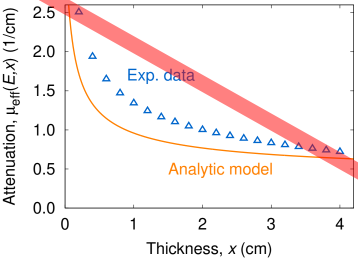

(∗) XCOM supplied by NIST

Numerical approx. of $\mu_{\mathrm{eff}}(x)$

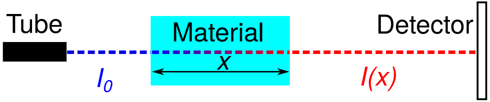

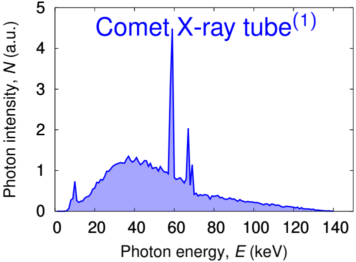

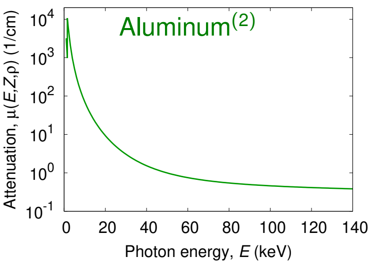

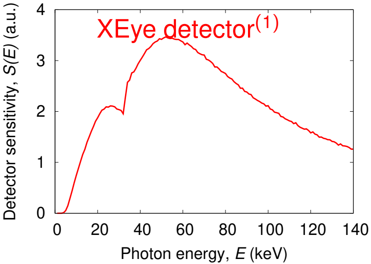

$$I(x) \propto \int N(E) \exp\{-\mu(E)x\} S(E)\, \mathrm{d}E$$

$$\int \rightarrow \sum$$

(1) Supplied by Norman Uhlmann, Fraunhofer EZRT

(2) XCOM supplied by NIST

Numerical approx. of $\mu_{\text{eff}}(x)$

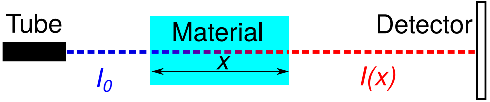

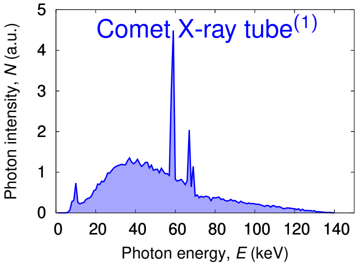

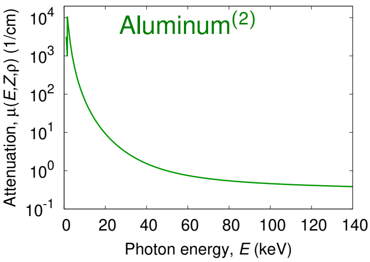

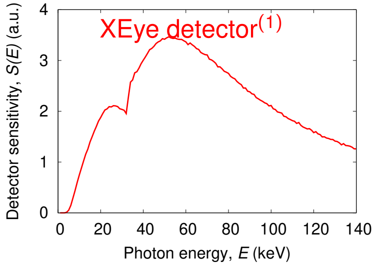

$$I(x) \propto \int N(E)\, \exp\{-\mu(E)x\}\, S(E)\, \mathrm{d}E$$

$$\int \rightarrow \sum$$

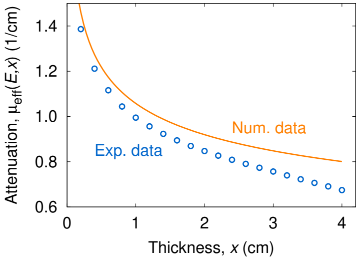

(1) Supplied by Norman Uhlmann, Fraunhofer EZRT

(2) XCOM supplied by NIST

Numerical approx. of $\mu_{\mathrm{eff}}(x)$

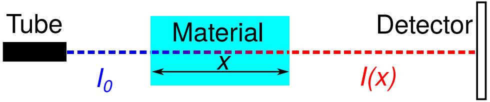

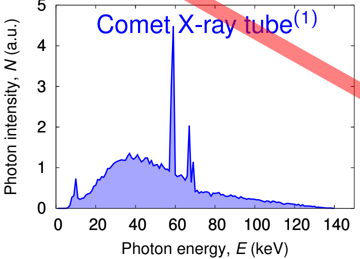

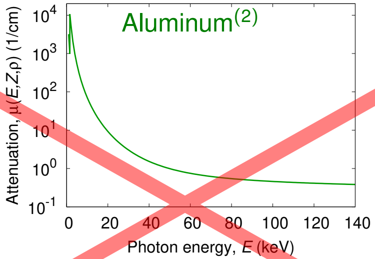

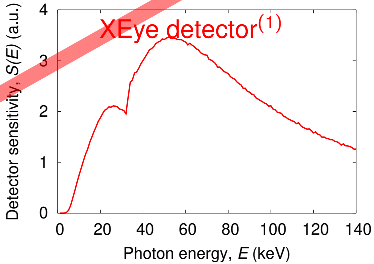

$$I(x) \propto \int N(E)\exp\{-\mu(E)x\}S(E)\,\mathrm{d}E$$

$$\int \to \sum$$

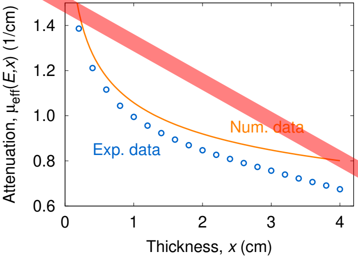

(1) Supplied by Norman Uhlmann, Fraunhofer EZRT

(2) XCOM supplied by NIST

Heuristic model functions for $\mu_{\text{eff}}(x)$

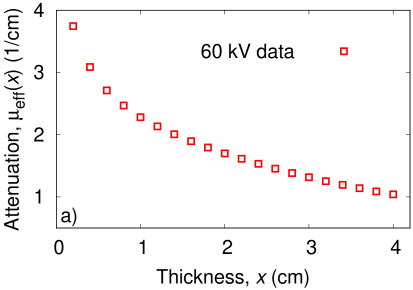

Heuristic model functions for $\mu_{\text{eff}}(x)$

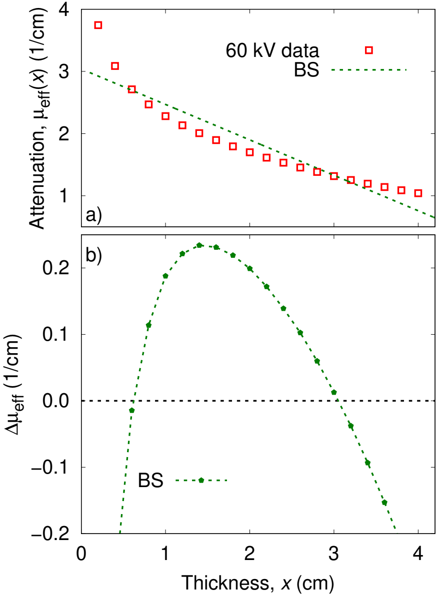

$$\mu_{\text{eff}}(x) = \mu_0 - \lambda x$$

Bjärngard & Shackford (1994)

Heuristic model functions for $\mu_{\text{eff}}(x)$

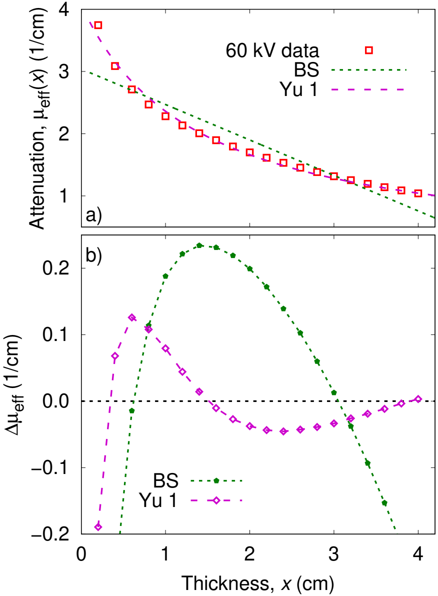

$$\mu_{\text{eff}}(x) = \mu_0 - \lambda x$$

Bjärngard & Shackford (1994)

$$\mu_{\text{eff}}(x) = \frac{\mu_0}{1+\lambda x}$$

Yu *et al.* (1997)

Heuristic model functions for $\mu_{\text{eff}}(x)$

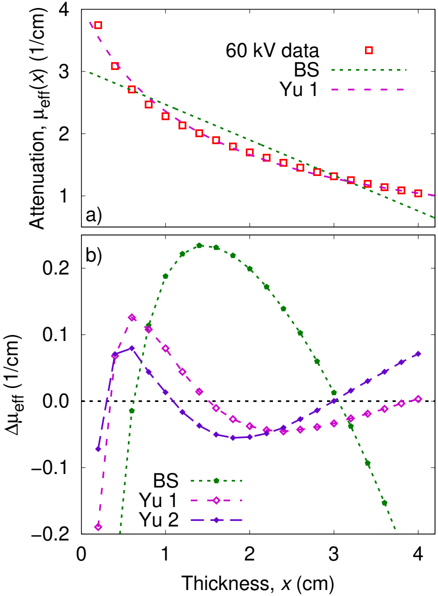

$$\mu_{\text{eff}}(x) = \mu_0 - \lambda x$$

Bjärngard & Shackford (1994)

$$\mu_{\text{eff}}(x) = \frac{\mu_0}{1+\lambda x}$$

$$\mu_{\text{eff}}(x) = \frac{\mu_0}{(1+\lambda x)^\beta}$$

Yu *et al.* (1997)

Heuristic model functions for $\mu_{\text{eff}}(x)$

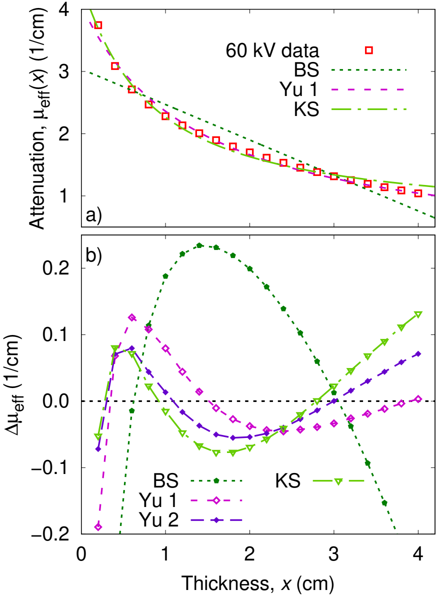

$$\mu_{\text{eff}}(x) = \mu_0 - \lambda x$$

Bjärngard & Shackford (1994)

$$\mu_{\text{eff}}(x) = \frac{\mu_0}{1+\lambda x}$$

$$\mu_{\text{eff}}(x) = \frac{\mu_0}{(1+\lambda x)^{\beta}}$$

Yu *et al.* (1997)

$$\mu_{\text{eff}}(x) = \mu(E_{\max}) + \frac{2\mu_1}{x\sqrt{-\lambda_1^2+4\lambda_2}} \times \left[\arctan\left(\frac{\lambda_1+2\lambda_2 x}{\sqrt{-\lambda_1^2+4\lambda_2}}\right) - \arctan\left(\frac{\lambda_1}{\sqrt{-\lambda_1^2+4\lambda_2}}\right)\right]$$

Kleinschmidt (1999)

Heuristic model functions for $\mu_{\text{eff}}(x)$

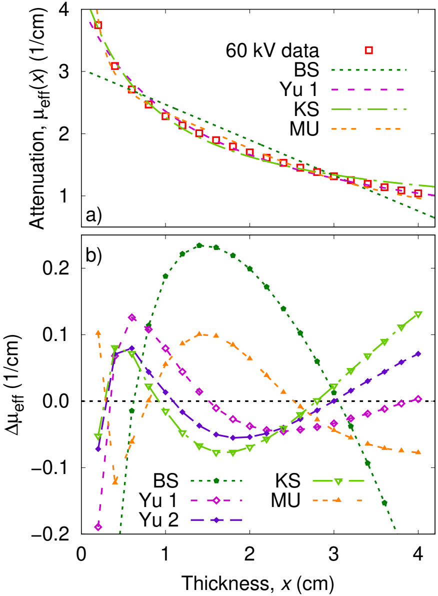

$$\mu_{\text{eff}}(x) = \mu_0 - \lambda x$$

Bjärngard & Shackford (1994)

$$\mu_{\text{eff}}(x) = \frac{\mu_0}{1+\lambda x}$$

$$\mu_{\text{eff}}(x) = \frac{\mu_0}{(1+\lambda x)^\beta}$$

Yu *et al.* (1997)

$$\mu_{\text{eff}}(x) = \mu(E_{\max}) + \frac{2\mu_1}{x\sqrt{-\lambda_1^2+4\lambda_2}} \times \left[\arctan\left(\frac{\lambda_1+2\lambda_2 x}{\sqrt{-\lambda_1^2+4\lambda_2}}\right) - \arctan\left(\frac{\lambda_1}{\sqrt{-\lambda_1^2+4\lambda_2}}\right)\right]$$

Kleinschmidt (1999)

$$\mu_{\text{eff}}(x) = -\frac{1}{x}\ln\left[A + B\exp(-x/C)\right]$$

Mudde *et al.* (2008)

Heuristic model functions for $\mu_{\text{eff}}(x)$

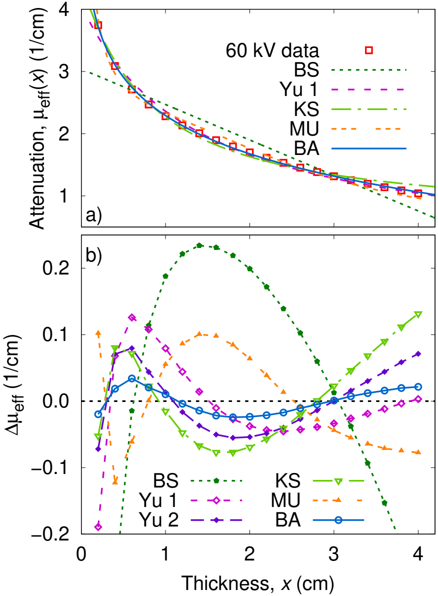

$$\mu_{\text{eff}}(x) = \mu_0 - \lambda x$$

Bjärngard & Shackford (1994)

$$\mu_{\text{eff}}(x) = \frac{\mu_0}{1+\lambda x}$$

$$\mu_{\text{eff}}(x) = \frac{\mu_0}{(1+\lambda x)^{\beta}}$$

Yu *et al.* (1997)

$$\mu_{\text{eff}}(x) = \mu(E_{\text{max}}) + \frac{2\mu_1}{x\sqrt{-\lambda_1^2+4\lambda_2}} \times \left[\arctan\left(\frac{\lambda_1+2\lambda_2 x}{\sqrt{-\lambda_1^2+4\lambda_2}}\right) - \arctan\left(\frac{\lambda_1}{\sqrt{-\lambda_1^2+4\lambda_2}}\right)\right]$$

Kleinschmidt (1999)

$$\mu_{\text{eff}}(x) = -\frac{1}{x}\ln\left[A + B\exp(-x/C)\right]$$

Mudde *et al.* (2008)

$$\boldsymbol{\mu_{\text{eff}}(x) = a + \frac{b}{x^{\alpha}}}$$

Baur *et al.* (2019)

(this work)

Applicability of $\mu_{\mathrm{eff}}(x) = a + \frac{b}{x^{\alpha}}$

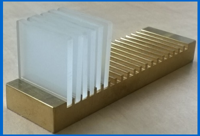

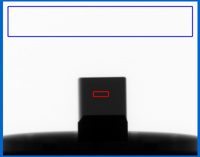

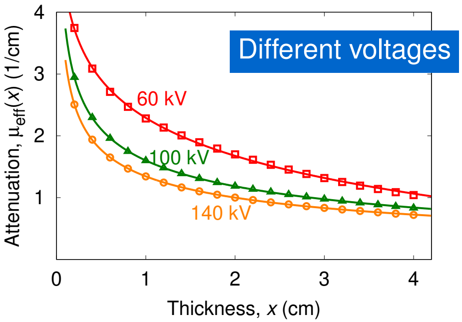

Applicability of $\mu_{\mathrm{eff}}(x) = a + \frac{b}{x^{\alpha}}$

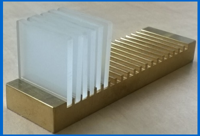

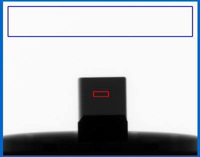

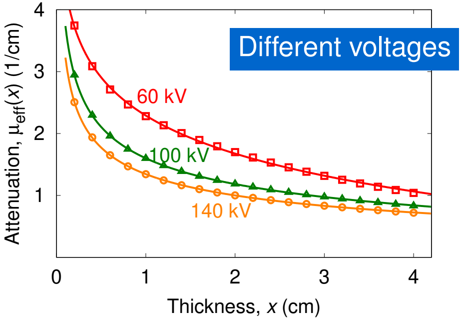

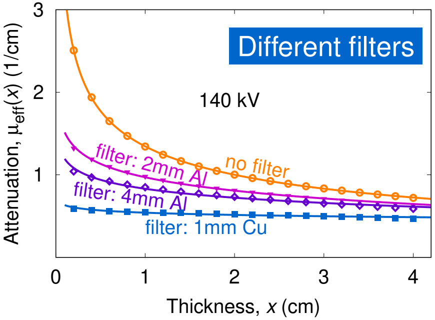

Applicability of $\mu_{\text{eff}}(x) = a + \frac{b}{x^{\alpha}}$

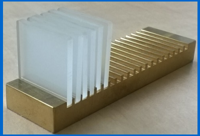

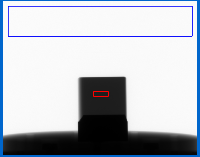

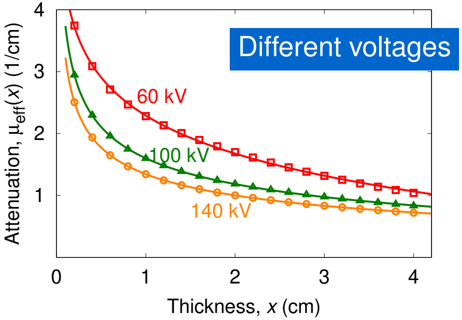

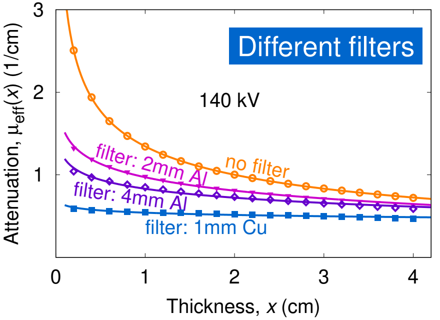

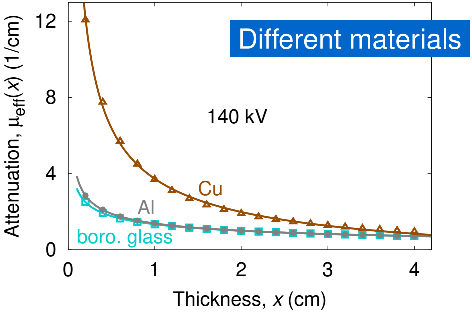

Applicability of $\mu_{\text{eff}}(x) = a + \frac{b}{x^{\alpha}}$

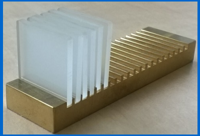

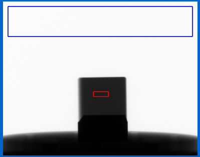

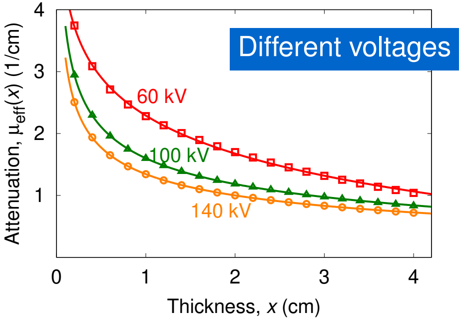

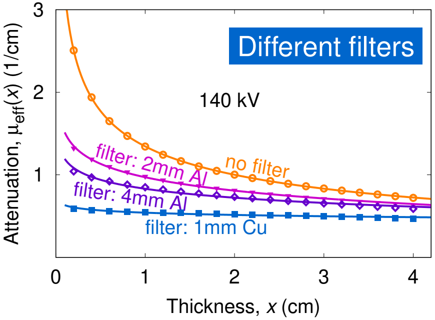

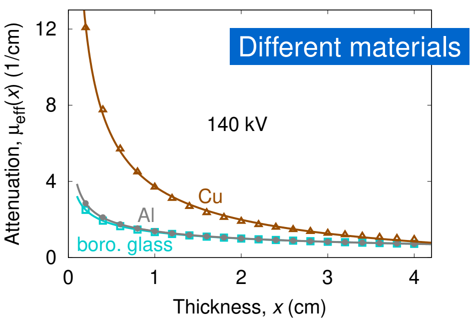

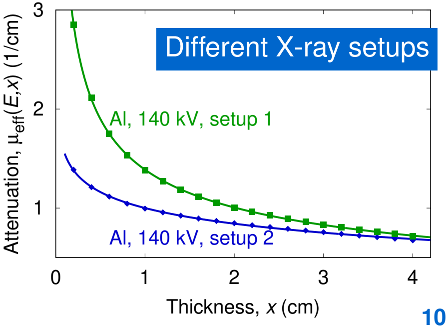

Determining the material thickness x

Generalized Beer-Lambert

$$I(x) = I_0 \exp(-\mu_{\text{eff}}(x)\, x)$$

Model function

$$\mu_{\text{eff}}(x) = a + \frac{b}{x^{\alpha}}$$

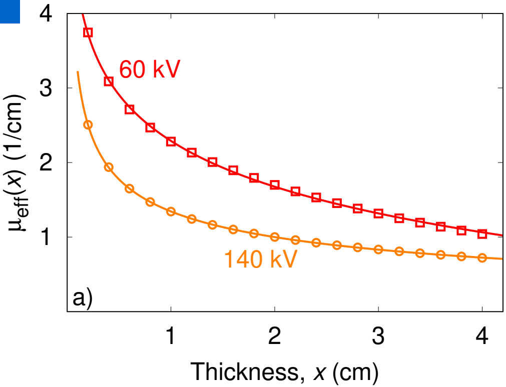

Determining the material thickness x

Generalized Beer-Lambert

$$I(x) = I_0 \exp(-\mu_{\text{eff}}(x)\, x)$$

Model function

$$\mu_{\text{eff}}(x) = a + \frac{b}{x^{\alpha}}$$

Solve

$$ax + bx^{1-\alpha} + \ln\left(\frac{I(x)}{I_0}\right) = 0$$

e.g. Newton's method or look-up table

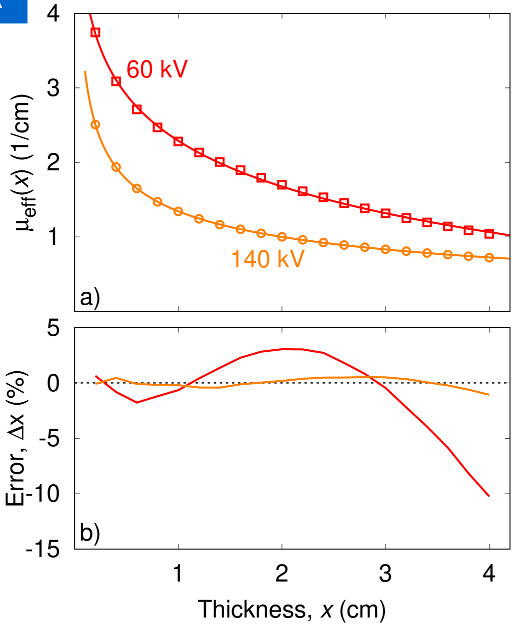

Determining the material thickness x

Generalized Beer-Lambert

$$I(x) = I_0 \exp(-\mu_{\text{eff}}(x)\, x)$$

Model function

$$\mu_{\text{eff}}(x) = a + \frac{b}{x^{\alpha}}$$

Solve

$$ax + bx^{1-\alpha} + \ln\left(\frac{I(x)}{I_0}\right) = 0$$

e.g. Newton's method or look-up table

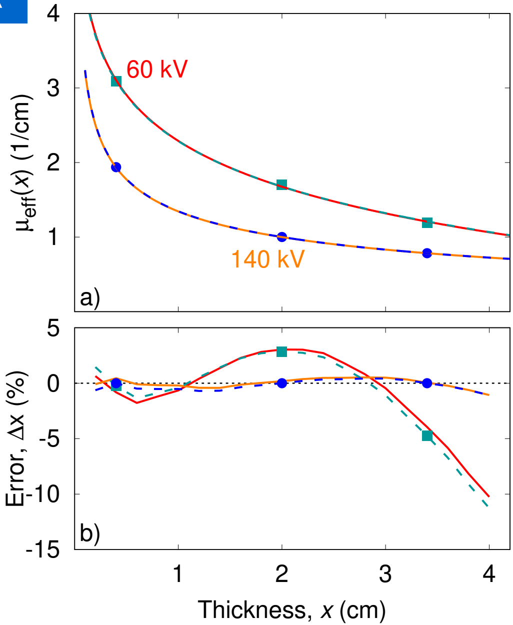

Migrating shear bands in shaken granular matter, Kollmer *et al* (2020)

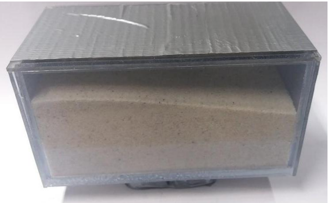

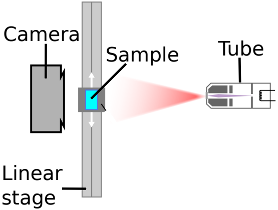

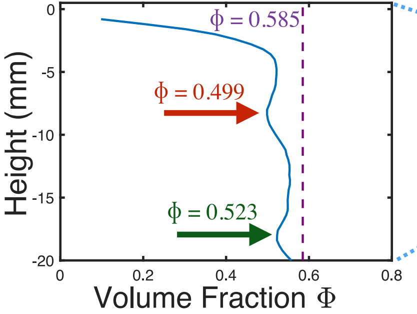

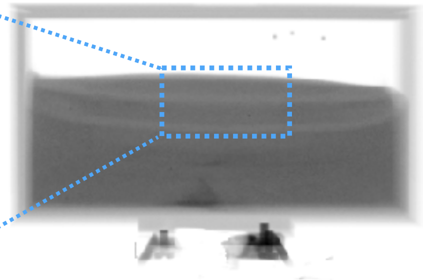

Measuring granular dynamics with X-ray Digital Fourier Analysis (X-DFA)

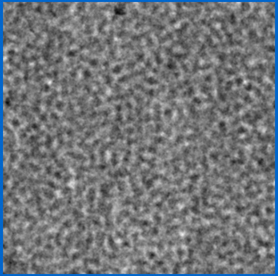

In collaboration with M. Escobedo & S. Egelhaaf, University of Düsseldorf

The system: A liquid fluidized bed

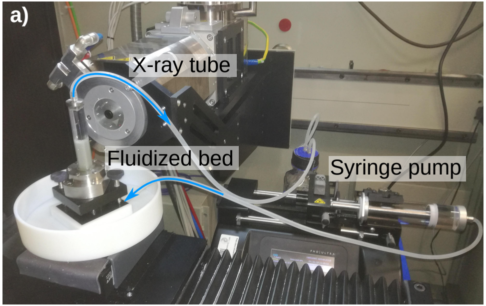

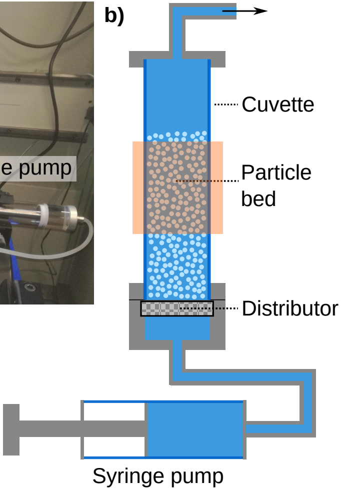

Radiogram

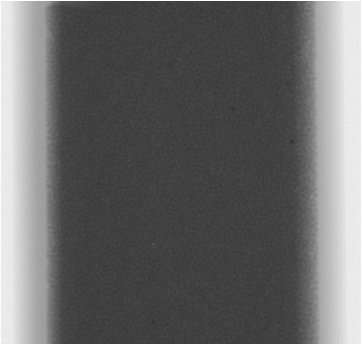

The system: A liquid fluidized bed

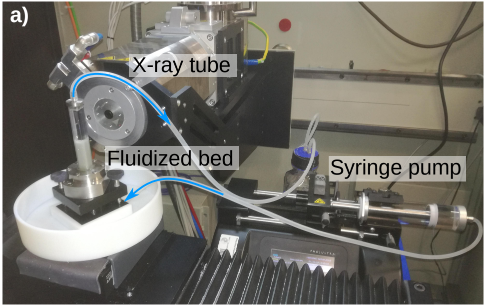

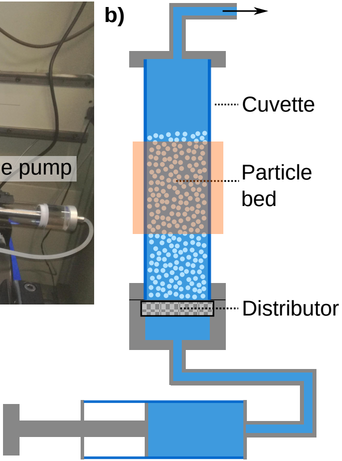

Particle tracking

Contrast: $\rho_{tracer} > \rho_{bed}$

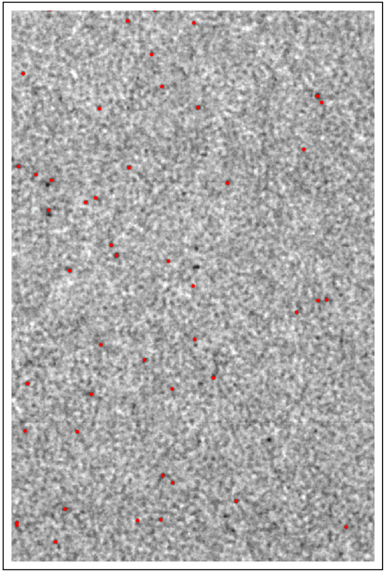

The system: A liquid fluidized bed

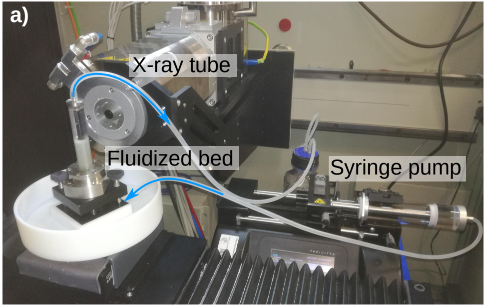

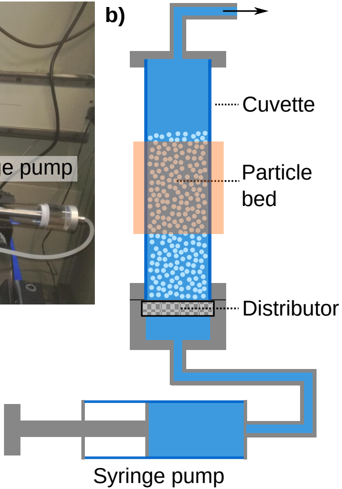

Particle tracking

Contrast: $\rho_{\mathrm{tracer}} > \rho_{\mathrm{bed}}$

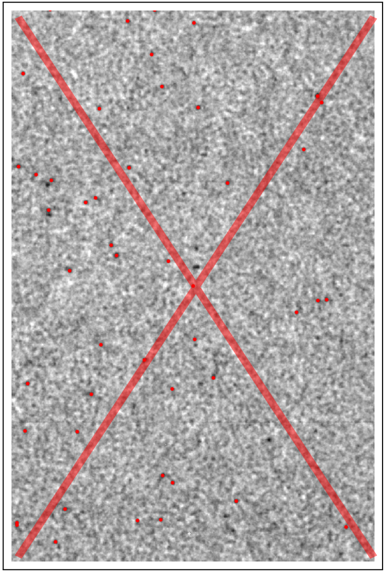

The system: A liquid fluidized bed

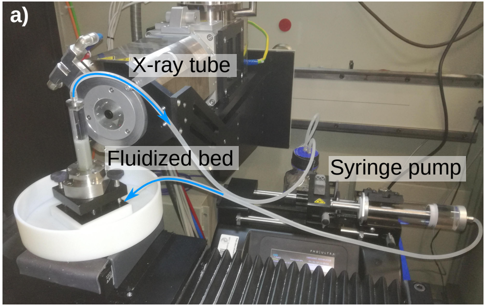

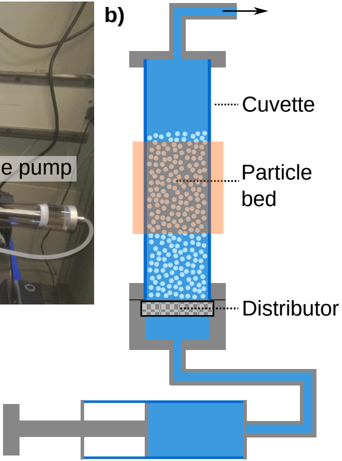

Radiogram

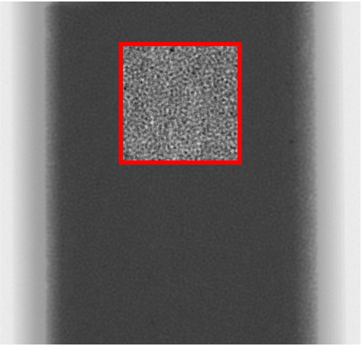

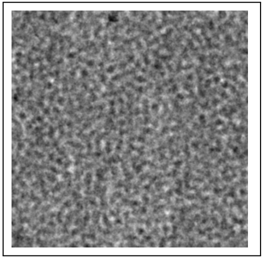

Differential Dynamic Microscopy (DDM)

	Up to now	**This work**
System	Dispersion, gels	Fluidized bed
Particles	Colloids < 1 µm	Granulates $(150 - 180)$ µm
Volume fraction	$\Phi \leq 0.33$	$0.45 < \Phi < 0.56$
Imaging	Light microscopy	X-ray radiography
Dynamics	Brownian motion, caging, glassy, collective motion	

Giavazzi *et al*, PRE **80**, 031403 (2009)

Extending Differential Dynamic Microscopy (DDM) to X-ray imaging

	Up to now	**This work**
System	Dispersion, gels	Fluidized bed
Particles	Colloids < 1 µm	Granulates $(150 - 180)$ µm
Volume fraction	$\Phi \leq 0.33$	$0.45 < \Phi < 0.56$
Imaging	Light microscopy	X-ray radiography
Dynamics	Brownian motion, caging, glassy, collective motion	

Digital Fourier Analysis of X-Ray radiograms (X-DFA)

Giavazzi *et al*, PRE **80**, 031403 (2009)

Introduction to X-ray Digital Fourier Analysis (X-DFA)

Synthetic radiograms

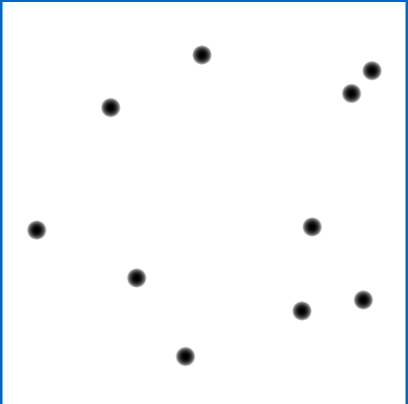

Particle trajectory

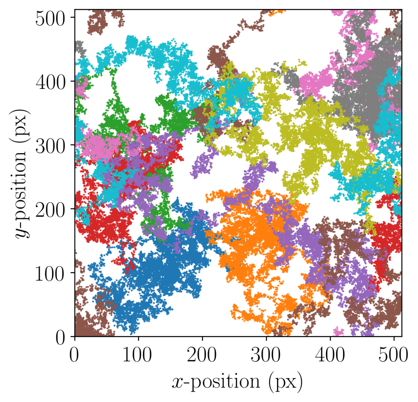

The image structure function $D(\mathbf{q}, \tau)$

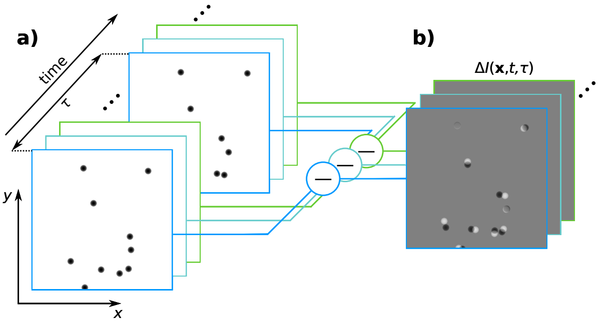

Giavazzi *et al*, PRE **80**, 031403 (2009)

The image structure function $D(\mathbf{q}, \tau)$

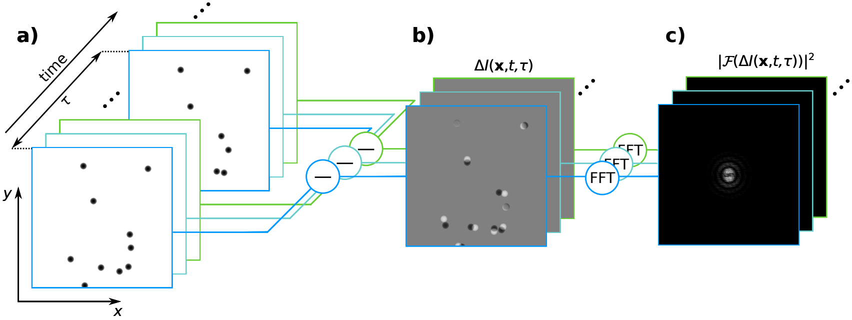

Giavazzi *et al*, PRE **80**, 031403 (2009)

The image structure function $D(\mathbf{q}, \tau)$

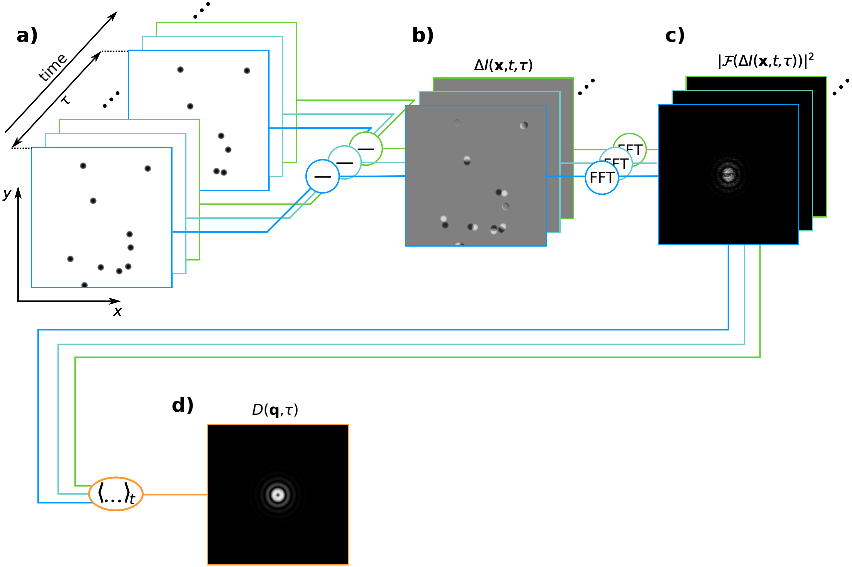

Giavazzi *et al*, PRE **80**, 031403 (2009)

The image structure function $D(\mathbf{q}, \tau)$

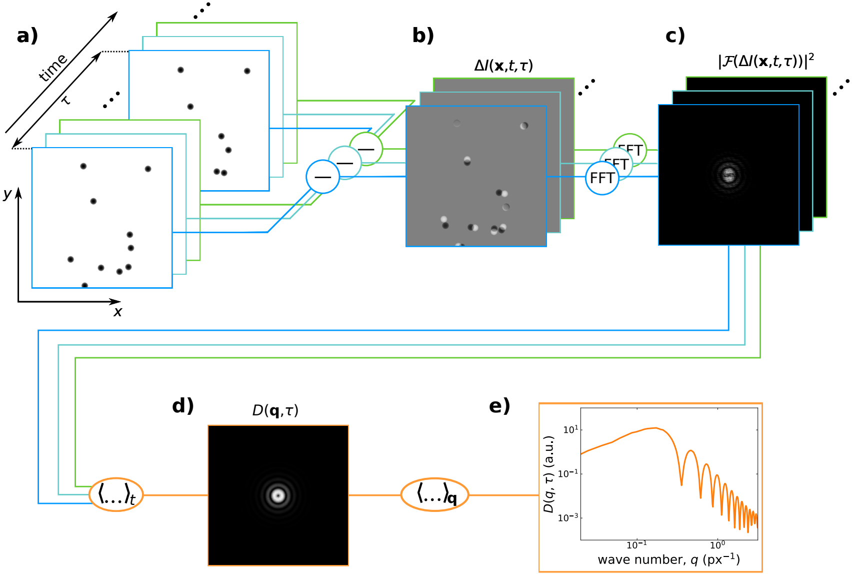

Giavazzi *et al*, PRE **80**, 031403 (2009)

The image structure function $D(q, \tau)$

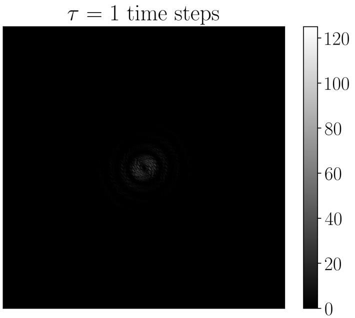

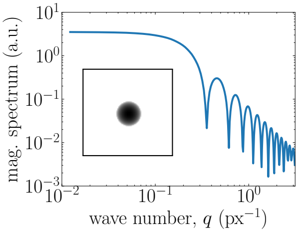

Time averaging: $D(\mathbf{q}, \tau) = \langle |\mathscr{F}(\Delta I)|^2 \rangle_t$

Azimuthal averaging: $D(\mathbf{q}, \tau) \rightarrow D(q, \tau)$ ...

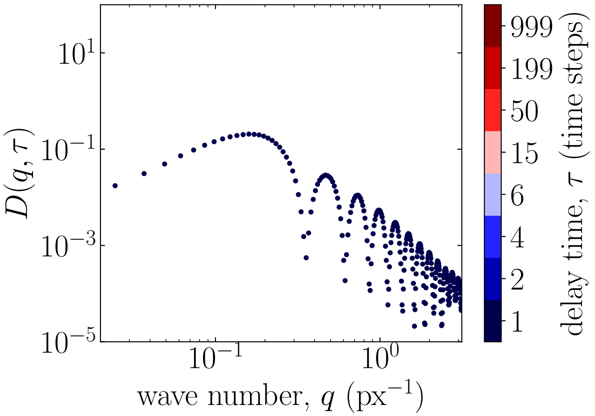

The image structure function $D(q, \tau)$

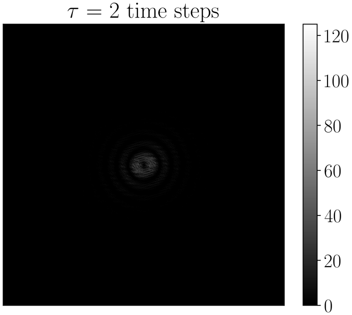

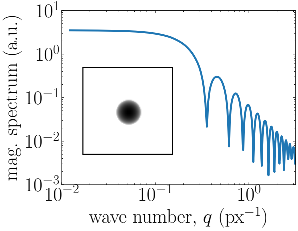

Time averaging: $D(\mathbf{q}, \tau) = \langle |\mathscr{F}(\Delta I)|^2 \rangle_t$

Azimuthal averaging: $D(\mathbf{q}, \tau) \rightarrow D(q, \tau)$ ...

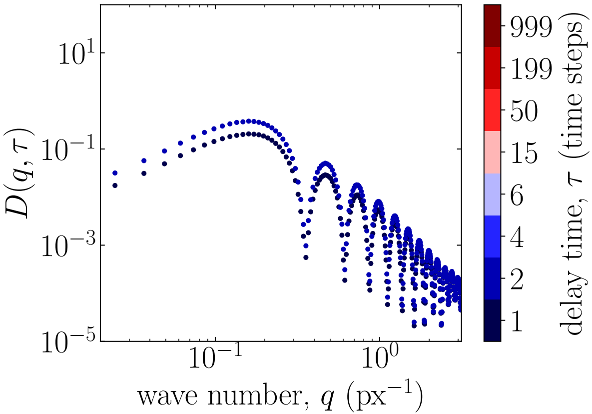

The image structure function $D(q, \tau)$

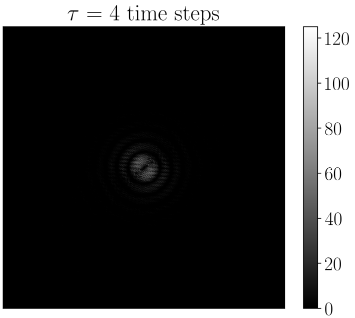

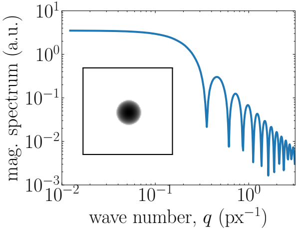

Time averaging: $D(\mathbf{q}, \tau) = \langle |\mathscr{F}(\Delta I)|^2 \rangle_t$

Azimuthal averaging: $D(\mathbf{q}, \tau) \to D(q, \tau)$ ...

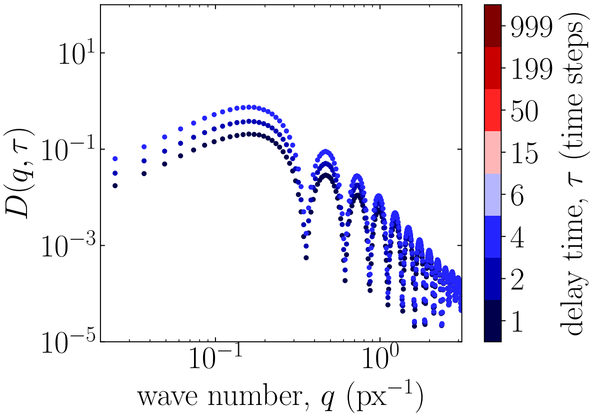

The image structure function $D(q, \tau)$

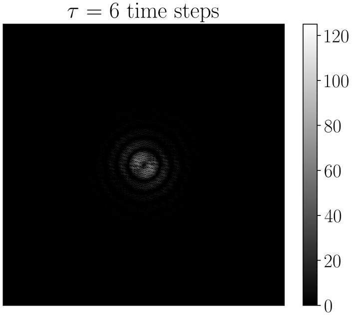

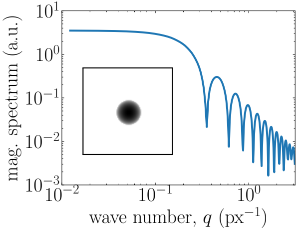

Time averaging: $D(\mathbf{q}, \tau) = \langle |\mathscr{F}(\Delta I)|^2 \rangle_t$

Azimuthal averaging: $D(\mathbf{q}, \tau) \rightarrow D(q, \tau)$ ...

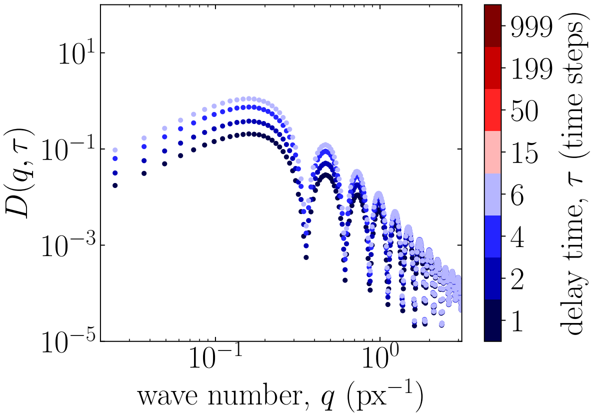

The image structure function $D(q, \tau)$

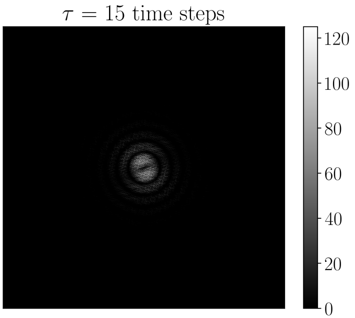

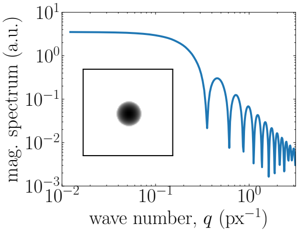

Time averaging: $D(\mathbf{q}, \tau) = \langle |\mathscr{F}(\Delta I)|^2 \rangle_t$

Azimuthal averaging: $D(\mathbf{q}, \tau) \rightarrow D(q, \tau)$ ...

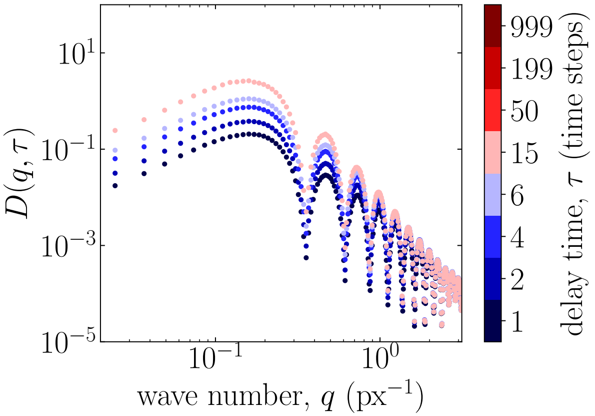

The image structure function $D(q, \tau)$

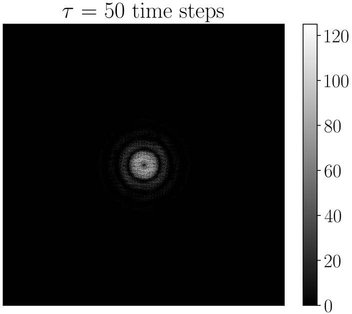

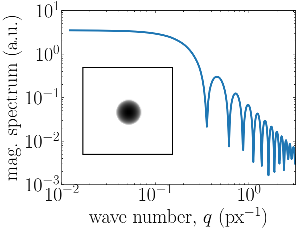

Time averaging: $D(\mathbf{q}, \tau) = \langle |\mathscr{F}(\Delta I)|^2 \rangle_t$

Azimuthal averaging: $D(\mathbf{q}, \tau) \rightarrow D(q, \tau)$ ...

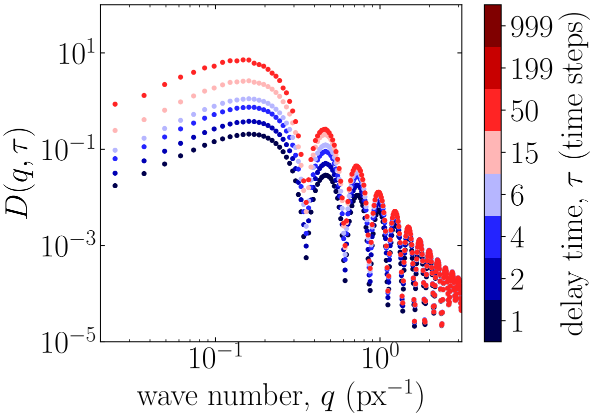

The image structure function $D(q, \tau)$

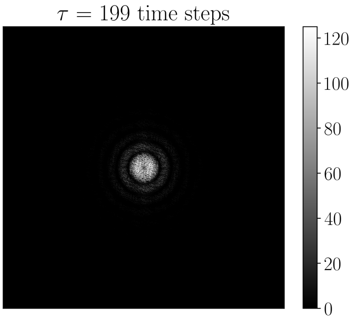

Time averaging: $D(\mathbf{q}, \tau) = \langle |\mathscr{F}(\Delta I)|^2 \rangle_t$

Azimuthal averaging: $D(\mathbf{q}, \tau) \rightarrow D(q, \tau)$ ...

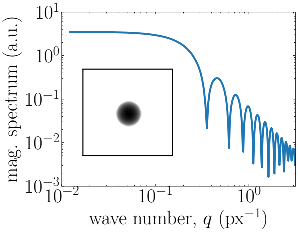

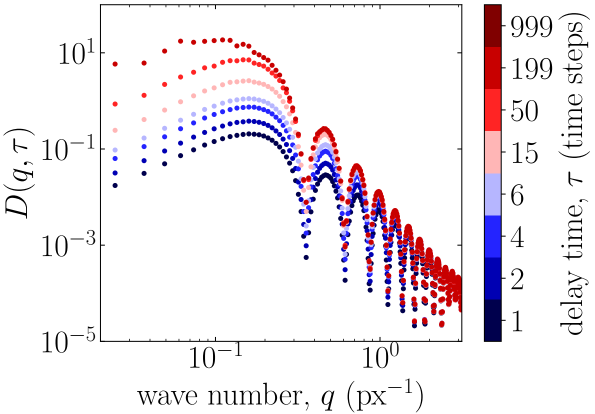

The image structure function $D(q, \tau)$

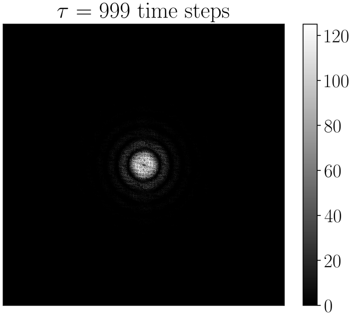

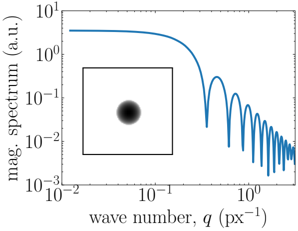

Time averaging: $D(\mathbf{q}, \tau) = \langle |\mathscr{F}(\Delta I)|^2 \rangle_t$

Azimuthal averaging: $D(\mathbf{q}, \tau) \rightarrow D(q, \tau)$ ...

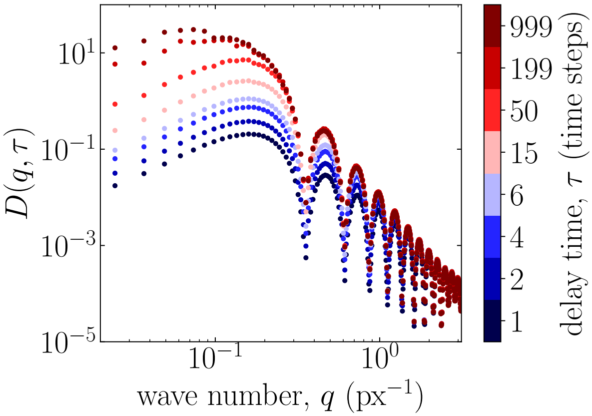

The image structure function $D(q, \tau)$

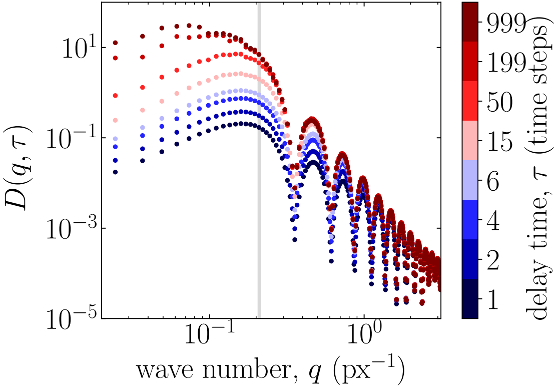

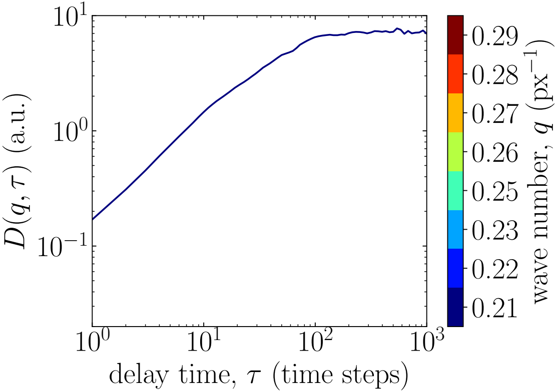

The image structure function $D(q, \tau)$

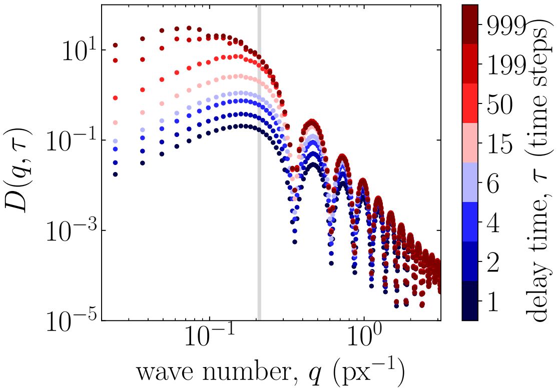

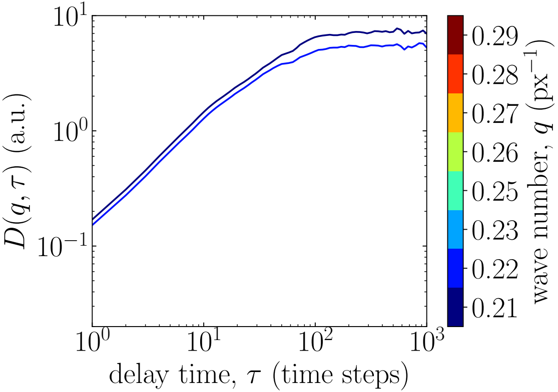

The image structure function $D(q, \tau)$

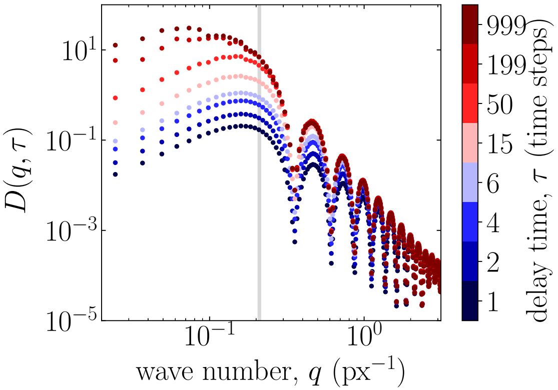

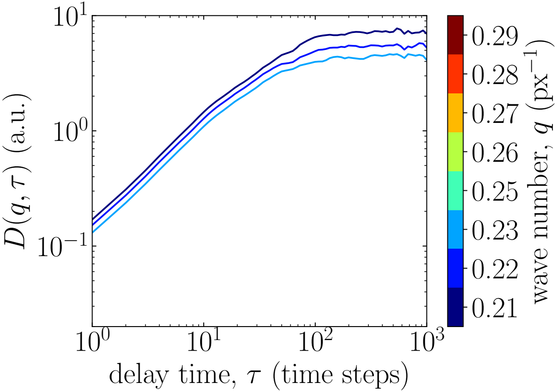

The image structure function $D(q, \tau)$

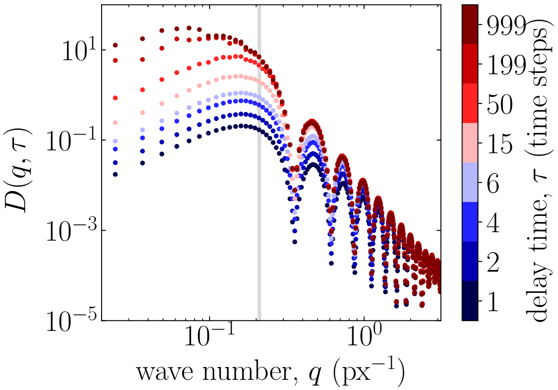

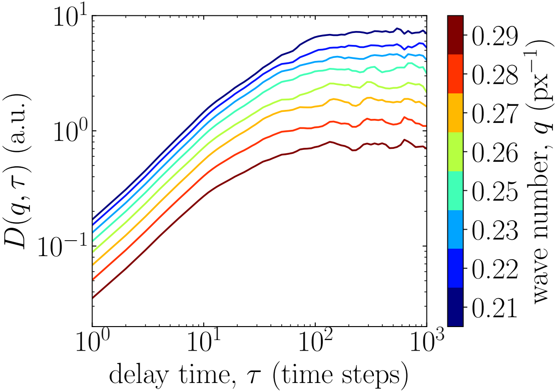

Linear space invariant imaging

$$D(q, \tau) = \left\langle \left| I(q, t + \tau) - I(q, t) \right|^2 \right\rangle_t$$

Linear space invariant imaging

$$D(q,\tau) = \left\langle |I(q,t+\tau) - I(q,t)|^2 \right\rangle_t$$

$$= A(q)\left[1 - \frac{\left\langle I^*(q,t)I(q,t+\tau)\right\rangle_t}{\left\langle |I(q,t)|^2\right\rangle_t}\right] + B(q)$$

Linear space invariant imaging

$$D(q,\tau) = \left\langle |I(q,t+\tau) - I(q,t)|^2 \right\rangle_t$$

$$= A(q)\left[1 - \underbrace{\frac{\left\langle I^*(q,t)I(q,t+\tau)\right\rangle_t}{\left\langle |I(q,t)|^2\right\rangle_t}}_{\text{Image correlation function}}\right] + B(q)$$

Linear space invariant imaging

$$D(q,\tau) = \left\langle \left| I(q,t+\tau) - I(q,t) \right|^2 \right\rangle_t$$

$$= A(q)\left[1 - \underbrace{\frac{\left\langle I^*(q,t)I(q,t+\tau)\right\rangle_t}{\left\langle |I(q,t)|^2 \right\rangle_t}}_{\text{Image correlation function}}\right] + B(q)$$

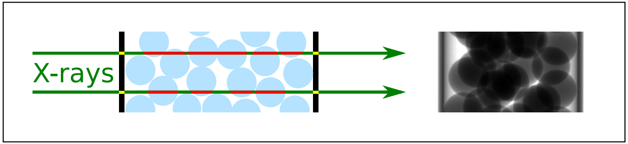

Intermediate scattering function

$$f(q,\tau) = \frac{\langle \rho^*(q,t)\rho(q,t+\tau)\rangle_t}{\langle |\rho(q,t)|^2\rangle_t}$$

Intermediate scattering function $f(q, \tau)$

Brownian motion: $f(q, \tau) = \exp(-q^2\tau/\tau_D)$

- Non-interacting particles
- Gaussian velocity distribution

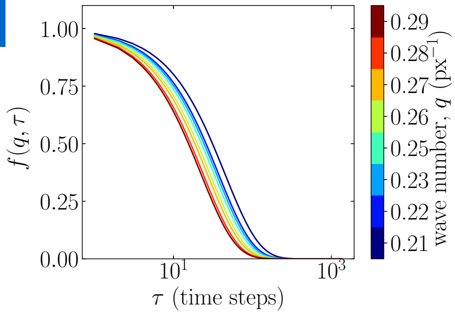

Intermediate scattering function $f(q, \tau)$

Brownian motion: $f(q, \tau) = \exp(-q^2\tau/\tau_\mathrm{D})$

- Non-interacting particles
- Gaussian velocity distribution

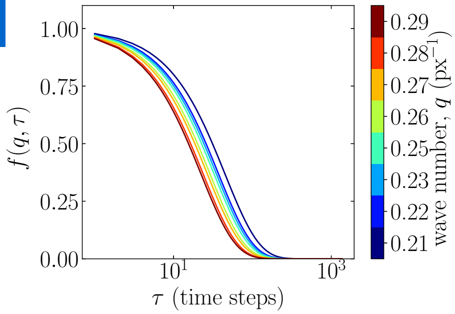

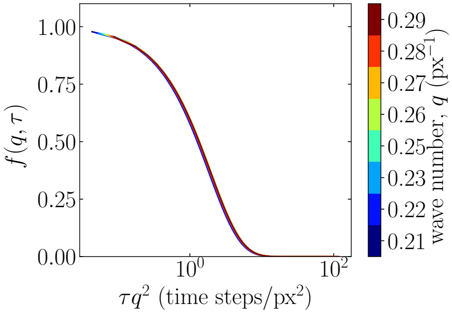

Intermediate scattering function $f(q, \tau)$

Brownian motion: $f(q, \tau) = \exp(-q^2\tau/\tau_\mathrm{D})$

- Non-interacting particles
- Gaussian velocity distribution

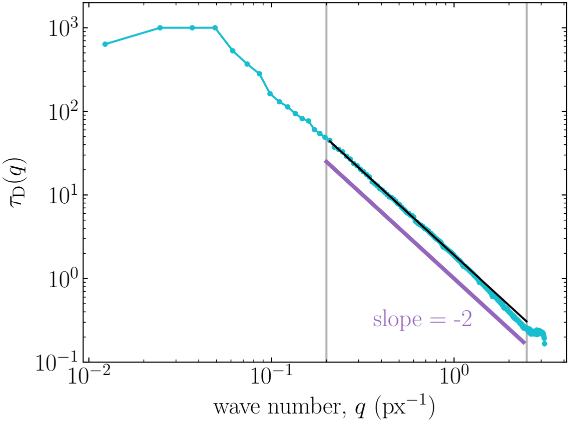

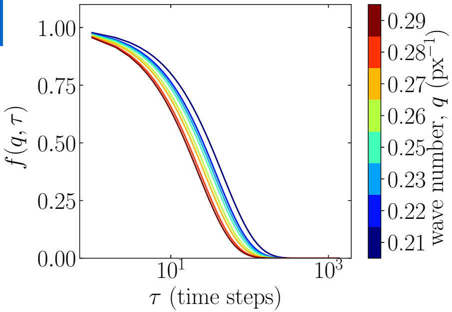

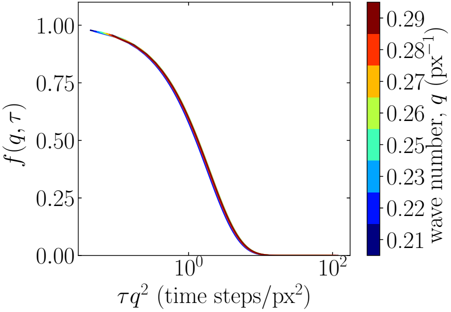

Accuracy of X-DFA: Varying the number of particles

10 particles

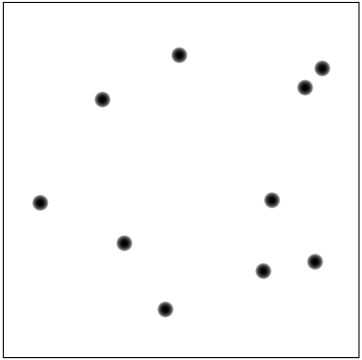

1000 particles

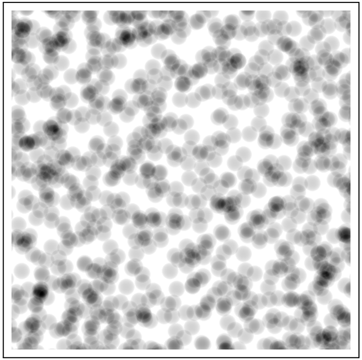

100 000 particles

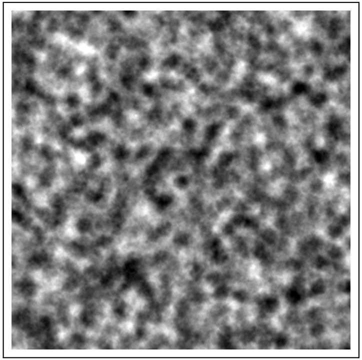

Deviation from the simulation input:

6%

2%

2%

PIV off by $\approx$ 650%

Experimental validation of X-DFA: A suspension of sedimenting particles

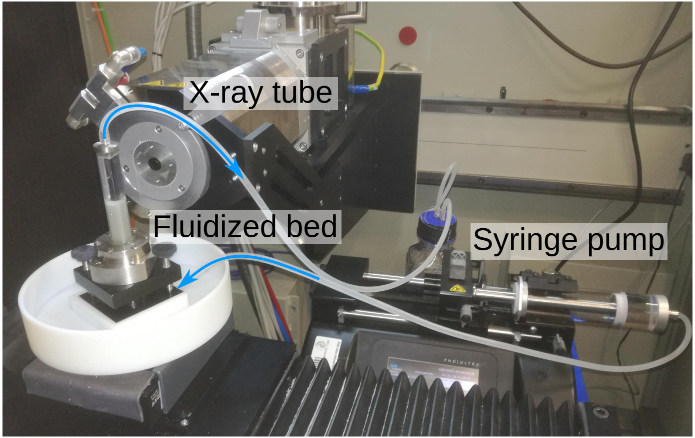

Experimental validation of X-DFA: A suspension of sedimenting particles

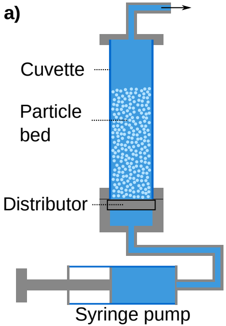

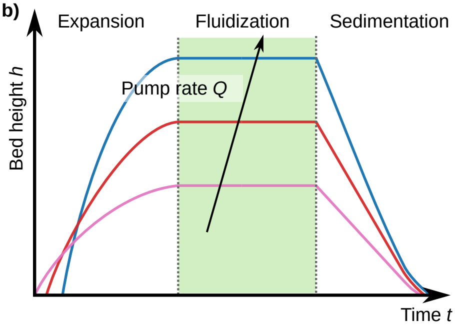

X-ray radiography

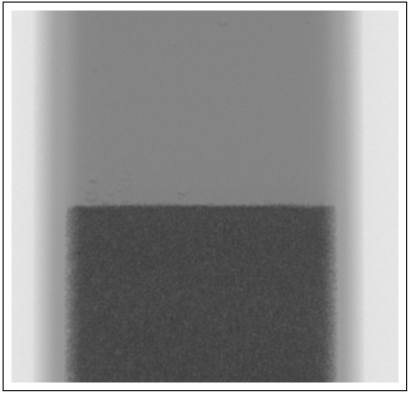

Experimental validation of X-DFA: A suspension of sedimenting particles

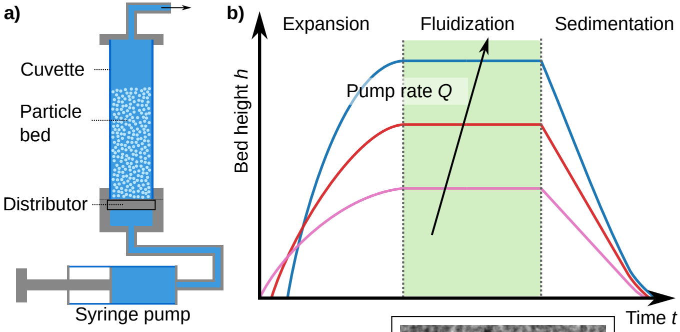

No reliable reference velocity!

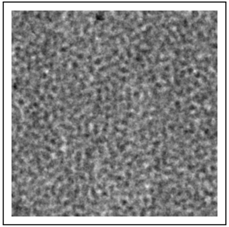

X-ray radiography

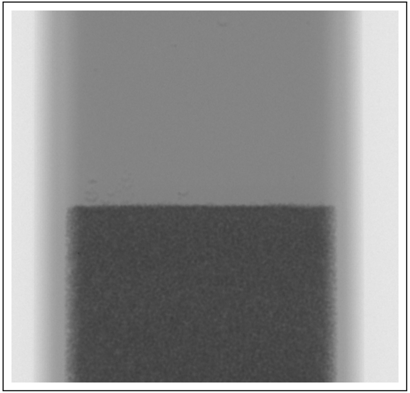

Experimental validation of X-DFA: A suspension of sedimenting particles

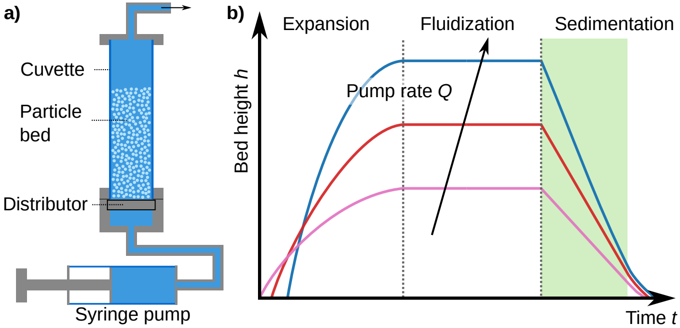

X-ray radiography

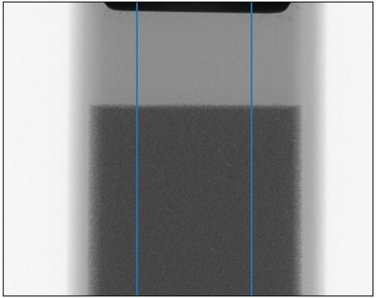

Experimental validation of X-DFA: A suspension of sedimenting particles

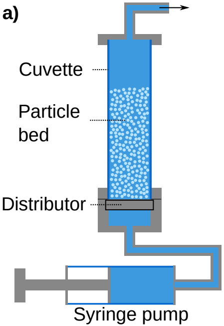

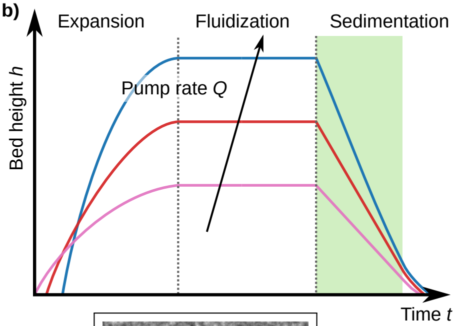

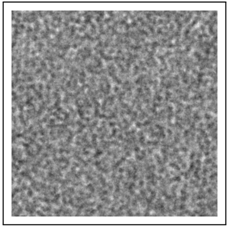

Comparison of $\langle v \rangle_{\mathrm{xdfa}}$ and $\langle v \rangle_{\mathrm{front}}$

X-ray radiography

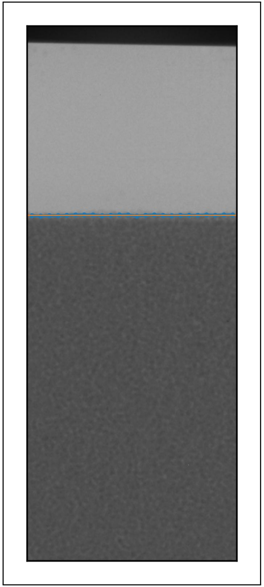

X-DFA for a suspension of sedimenting particles[1]

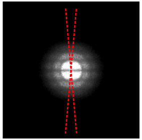

Image structure function:
$D(\mathbf{q}, \tau) = \langle |\mathcal{F}[\Delta I(\mathbf{r}, t, \tau)]|^2 \rangle_t$

(1) In collaboration with Manuel Escobedo, University of Düsseldorf

X-DFA for a suspension of sedimenting particles[1]

Intermediate scattering function[2]:

$$f(q,\tau) = \cos(q\langle v_s\rangle\tau)\exp\left(-\frac{1}{2}q^2\delta v^2\tau^2\right)$$

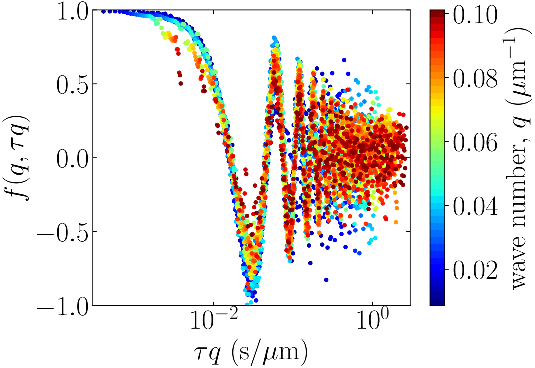

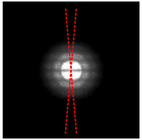

Image structure function:
$D(\mathbf{q},\tau) = \langle|\mathcal{F}[\Delta I(\mathbf{r},t,\tau)]|^2\rangle_t$

(1) In collaboration with Manuel Escobedo, University of Düsseldorf

(2) Kohyama *et al.* (2008)

X-DFA for a suspension of sedimenting particles[1]

Intermediate scattering function[2]:

$$f(q,\tau) = \cos(q\langle v_s\rangle\tau)\exp\left(-\frac{1}{2}q^2\delta v^2\tau^2\right)$$

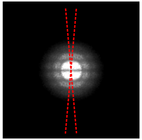

Image structure function:
$D(\mathbf{q},\tau) = \langle|\mathcal{F}[\Delta I(\mathbf{r},t,\tau)]|^2\rangle_t$

$\langle v_s\rangle = q\,\tau_\nu$ $\qquad \delta v = q\,\tau_{\delta\nu}$

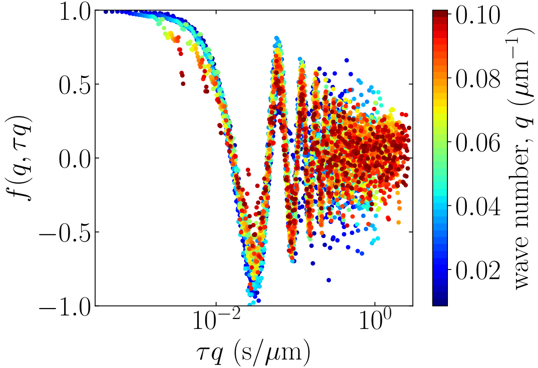

(1) In collaboration with Manuel Escobedo, University of Düsseldorf

(2) Kohyama *et al.* (2008)

X-DFA for a suspension of sedimenting particles[1]

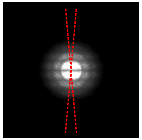

Image structure function:
$D(\mathbf{q},\tau) = \langle |\mathcal{F}[\Delta I(\mathbf{r},t,\tau)]|^2 \rangle_t$

Intermediate scattering function[2]:

$$f(q,\tau) = \cos(q\langle v_s \rangle \tau)\exp\left(-\frac{1}{2}q^2\delta v^2\tau^2\right)$$

$\langle v_s \rangle = q\,\tau_\nu \qquad \delta v = q\,\tau_{\delta\nu}$

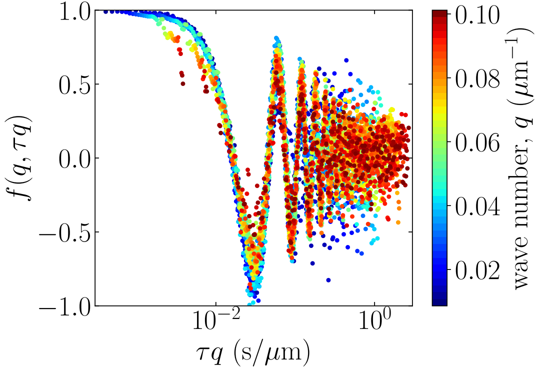

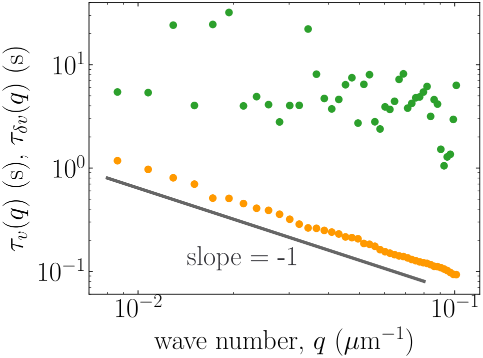

(1) In collaboration with Manuel Escobedo, University of Düsseldorf

(2) Kohyama *et al.* (2008)

Front tracking vs. X-DFA

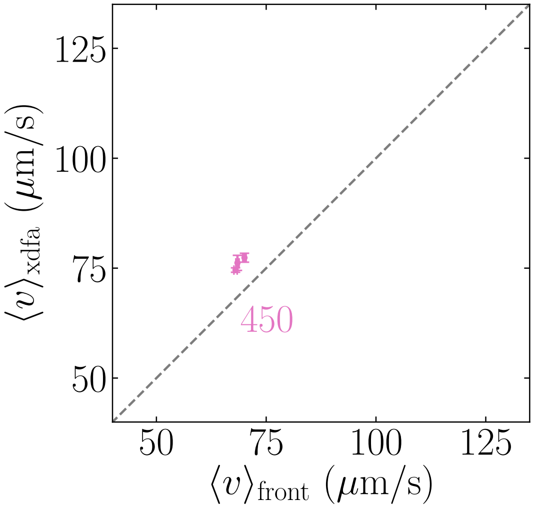

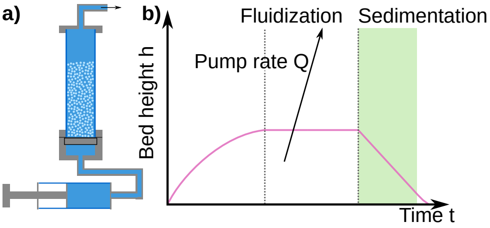

Front tracking vs. X-DFA

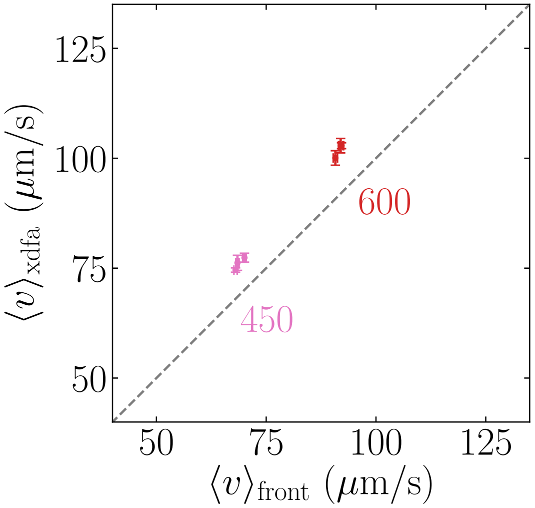

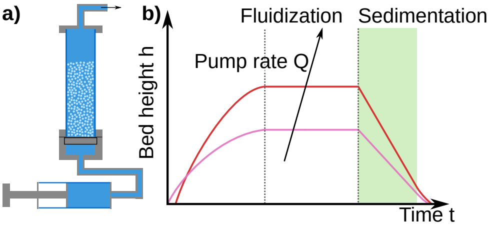

Front tracking vs. X-DFA

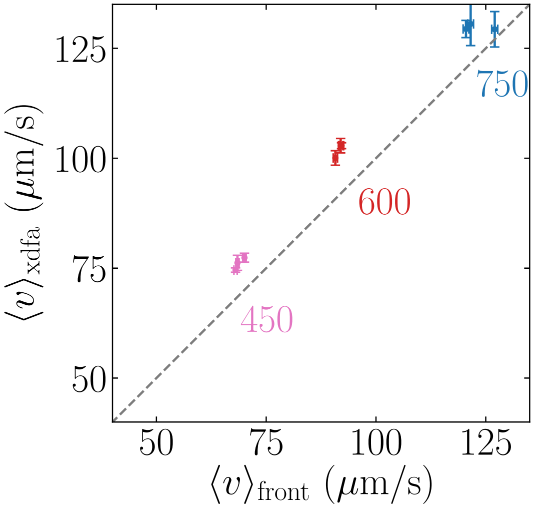

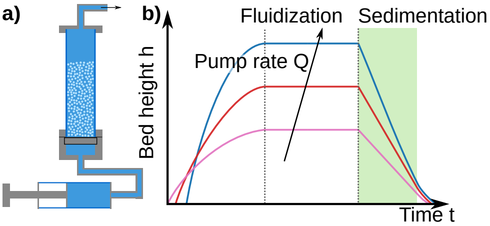

Front tracking vs. X-DFA

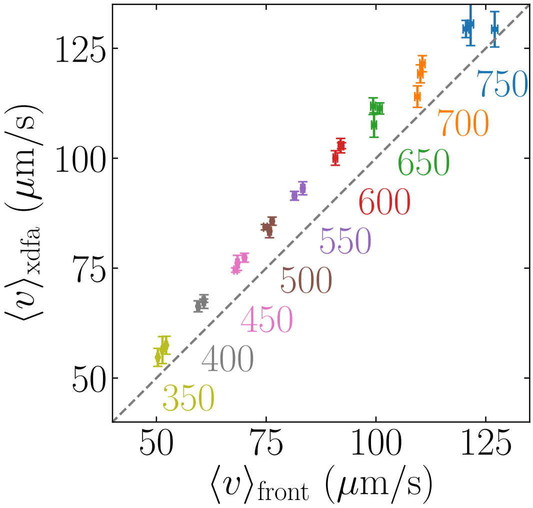

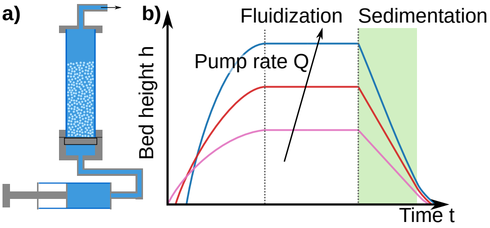

$\langle v \rangle_{\text{xdfa}} > \langle v \rangle_{\text{front}}$ by 9.4%

Front tracking vs. X-DFA

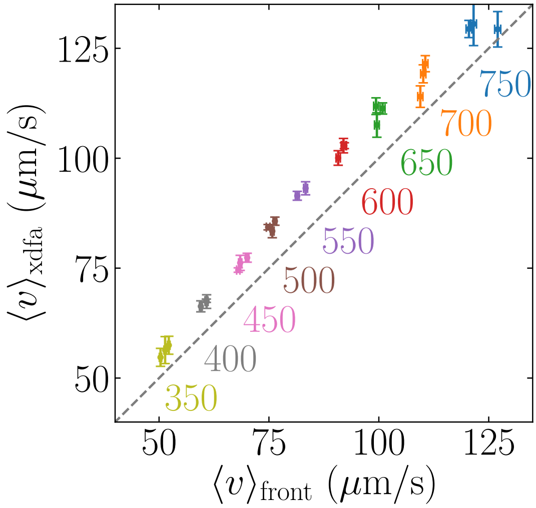

$\langle v \rangle_{\mathrm{xdfa}} > \langle v \rangle_{\mathrm{front}}$ by 9.4%

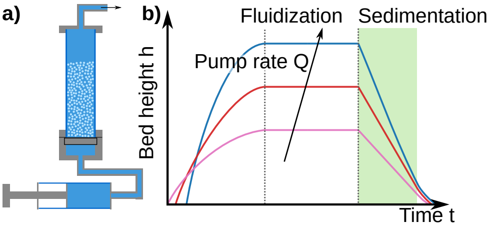

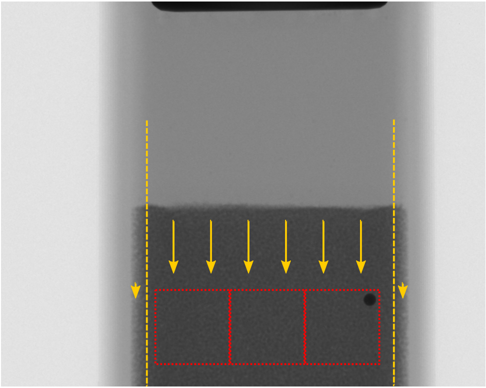

Correction of beam hardening

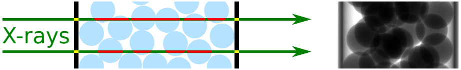

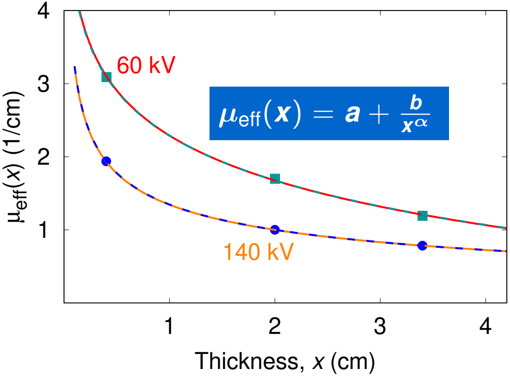

Conclusion

Correction of beam hardening

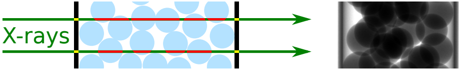

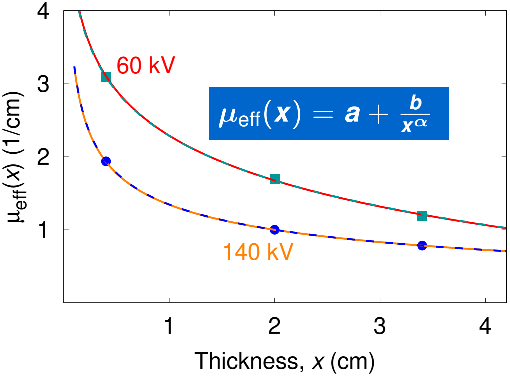

X-ray Digital Fourier Analysis

Synthetic radiograms

~~Particle Tracking~~

~~PIV~~

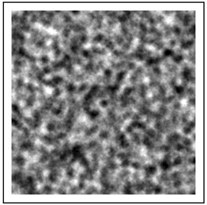

Experimental validation

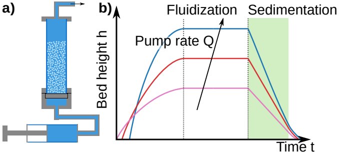

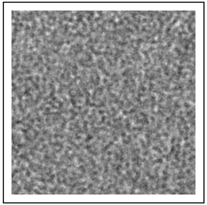

Conclusion

Correction of beam hardening

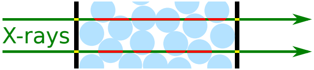

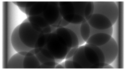

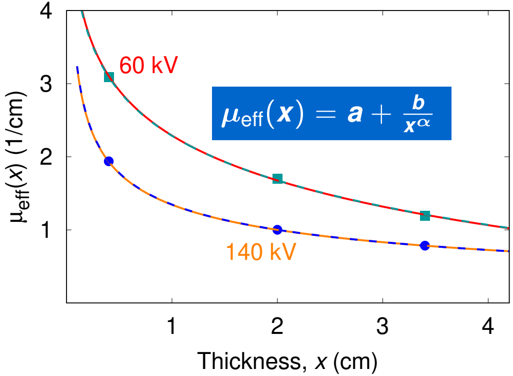

X-ray Digital Fourier Analysis

Synthetic radiograms

~~Particle Tracking~~

~~PIV~~

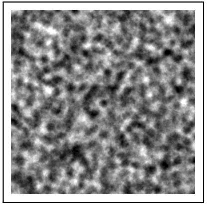

Experimental validation

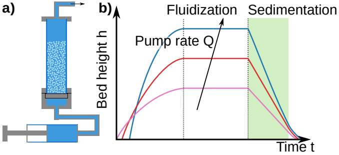

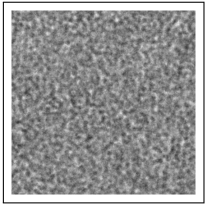

Temporal resolution of X-ray radiography

Thank you for your attention!

Backup slides

Synthetic radiograms

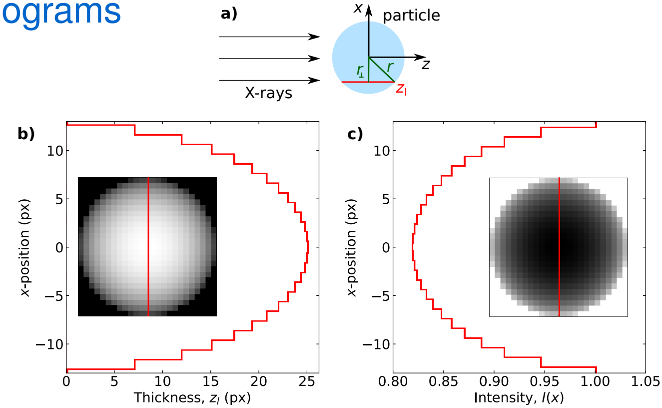

Beer-Lambert

$$I(z_l) = I_0 \exp(-\mu z)$$

Synthetic radiograms

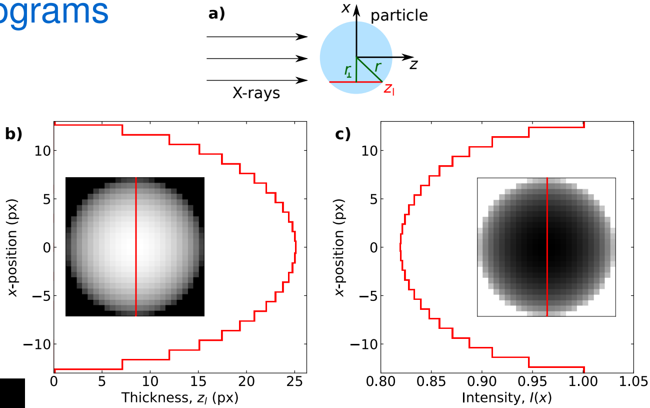

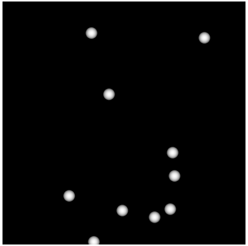

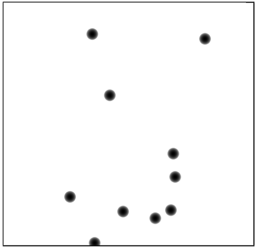

Beer-Lambert

$$I(z_l) = I_0 \exp(-\mu z)$$

Linear space invariant imaging

Image correlation function

$$g(\mathbf{q}, \tau) = \frac{\langle I^*(\mathbf{q}, t) I(\mathbf{q}, t + \tau) \rangle_t}{\langle |I(\mathbf{q}, t)|^2 \rangle_t}$$

Linear space invariant imaging

Image correlation function

$$g(\mathbf{q},\tau) = \frac{\langle I^*(\mathbf{q},t)I(\mathbf{q},t+\tau)\rangle_t}{\langle |I(\mathbf{q},t)|^2\rangle_t}$$

Intermediate scattering function

$$f(\mathbf{q},\tau) = \frac{\langle \rho^*(\mathbf{q},t)\rho(\mathbf{q},t+\tau)\rangle_t}{\langle |\rho(\mathbf{q},t)|^2\rangle_t}$$

Linear space-invariant imaging:

$$I(\mathbf{r},t) = I_0 + \int \mathrm{d}\mathbf{r}'\,\mathrm{d}z'\,T(\mathbf{r}-\mathbf{r}',-z')c(\mathbf{r}',z',t)$$

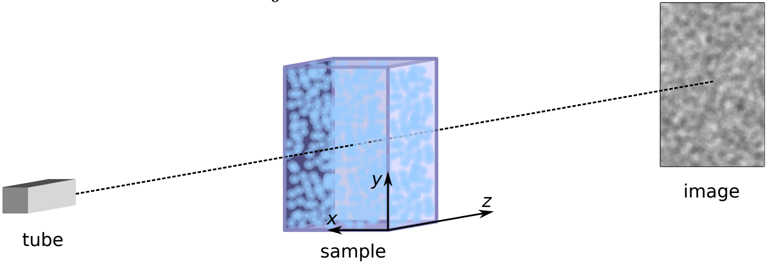

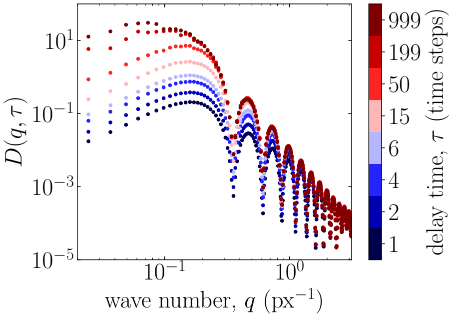

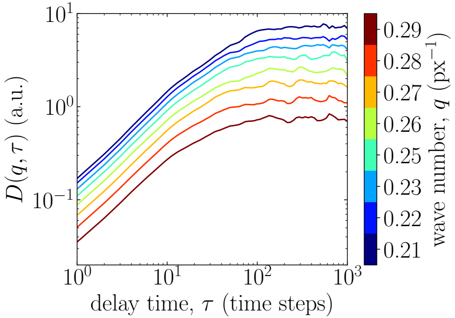

$$D(q,\tau) = \left\langle \left| I(q, t+\tau) - I(q,t) \right|^2 \right\rangle_t$$

$$= A(q)\left[1 - \underbrace{\frac{\left\langle I^*(q,t) I(q,t+\tau)\right\rangle_t}{\left\langle |I(q,t)|^2 \right\rangle_t}}_{\text{Image correlation function}}\right] + B(q)$$

Linear space invariant imaging

$$f(q,\tau) = \frac{\langle \rho^*(q,t)\rho(q,t+\tau)\rangle_t}{\langle |\rho(q,t)|^2\rangle_t}$$

Intermediate scattering function

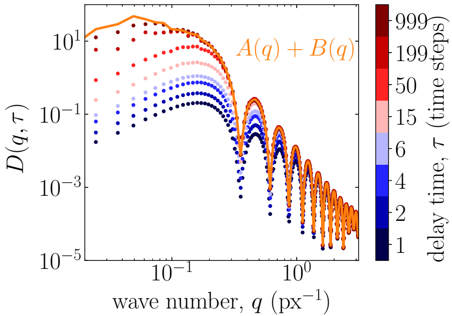

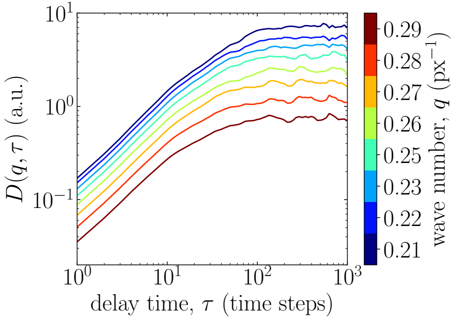

$$D(q,\tau) = \left\langle |I(q,t+\tau) - I(q,t)|^2 \right\rangle_t$$

$$= A(q)\left[1 - \frac{\langle I^*(q,t) I(q,t+\tau)\rangle_t}{\langle |I(q,t)|^2\rangle_t}\right] + B(q)$$

- $D(q,\tau \to 0) = B(q) = 0$
- $D(q,\tau \to \infty) = A(q) + B(q)$

Linear space invariant imaging

$$f(q,\tau) = \frac{\langle \rho^*(q,t)\rho(q,t+\tau)\rangle_t}{\langle |\rho(q,t)|^2\rangle_t}$$

Intermediate scattering function

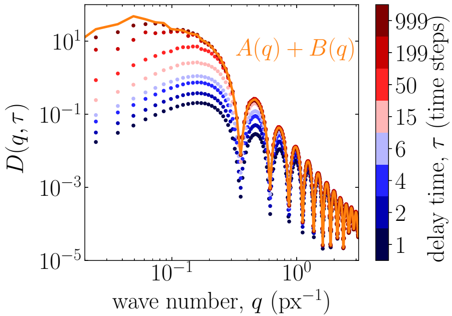

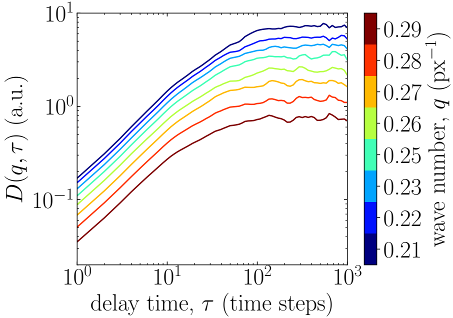

$$D(q,\tau) = \left\langle |I(q,t+\tau) - I(q,t)|^2 \right\rangle_t$$

$$= A(q)\left[1 - \frac{\langle I^*(q,t)I(q,t+\tau)\rangle_t}{\langle |I(q,t)|^2\rangle_t}\right] + B(q)$$

- $D(q,\tau \to 0) = B(q) = 0$
- $D(q,\tau \to \infty) = A(q) + B(q)$

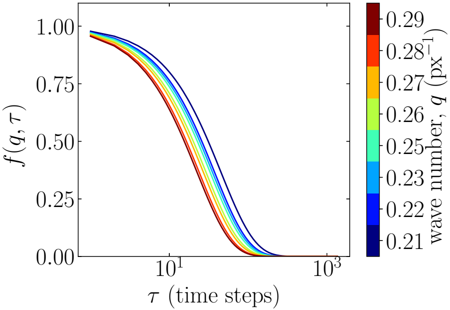

Experimental validation of X-DFA: A suspension of sedimenting particles

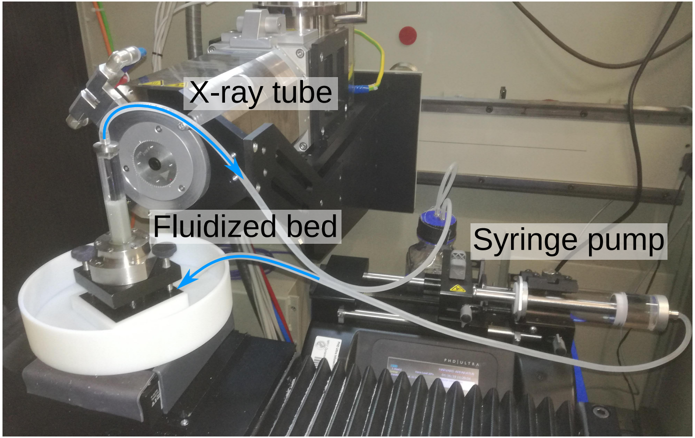

Experimental validation of X-DFA: A suspension of sedimenting particles

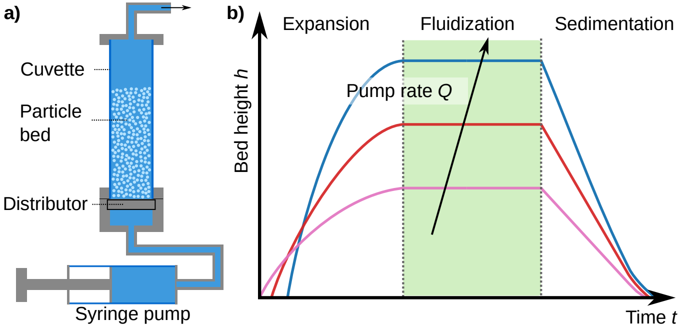

X-ray radiography

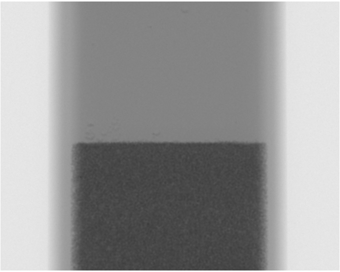

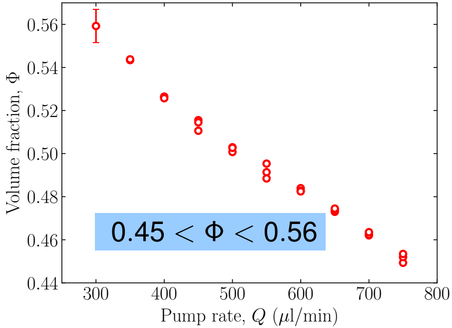

Liquid fluidized bed: Richardson-Zaki law

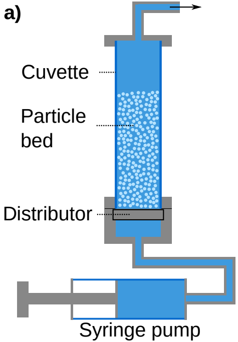

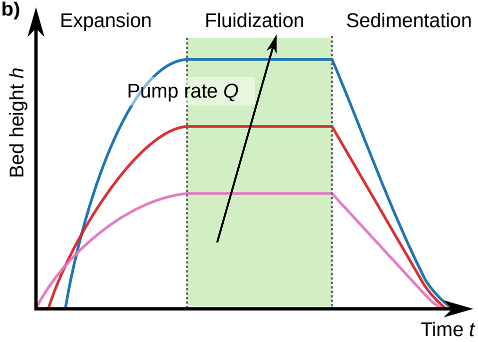

Gravitation Buoyancy Drag

$$F_G = F_B + F_D$$

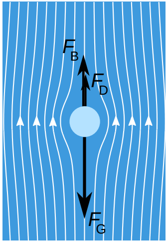

$$\frac{\langle v \rangle_{\text{fluid}}}{v_{\text{Stokes}}} = (1 - \Phi)^n$$

Liquid fluidized bed: Richardson-Zaki law

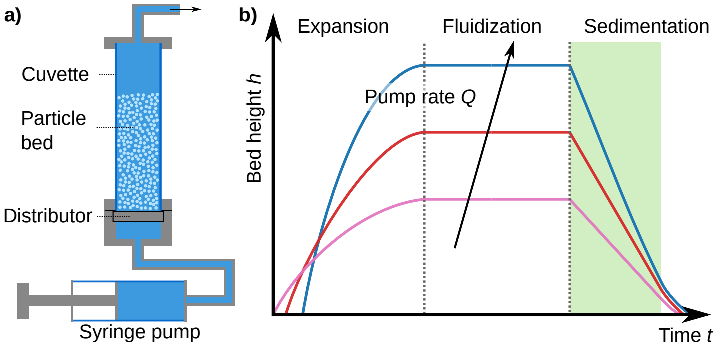

Gravitation Buoyancy Drag

$$F_G = F_B + F_D$$

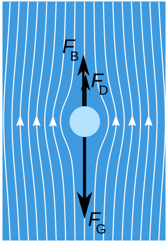

$$\frac{\langle v \rangle_{front}}{v_{Stokes}} = (1 - \Phi)^n$$

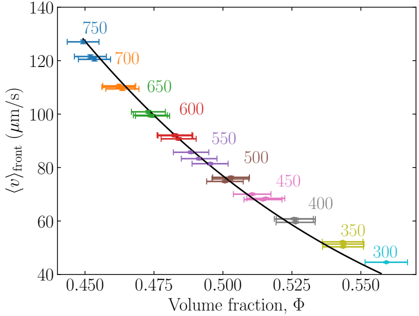

Tracking of particle front

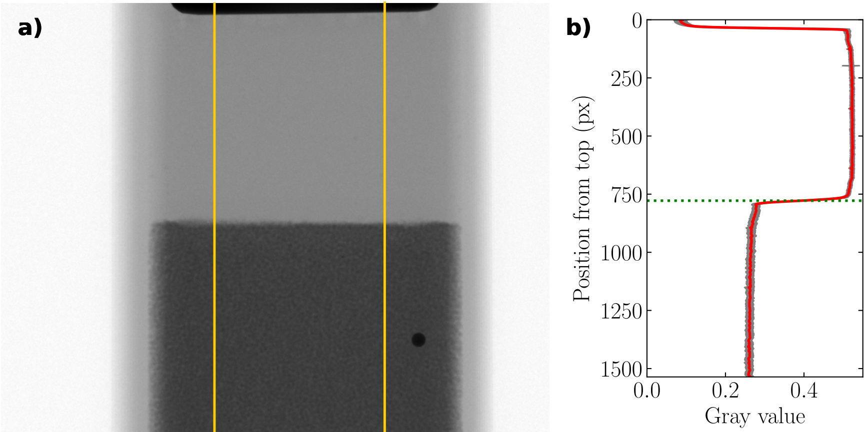

Tracking of particle front

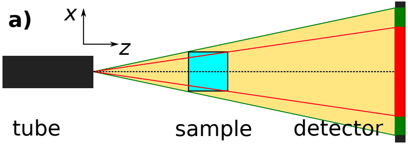

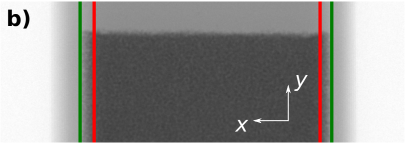

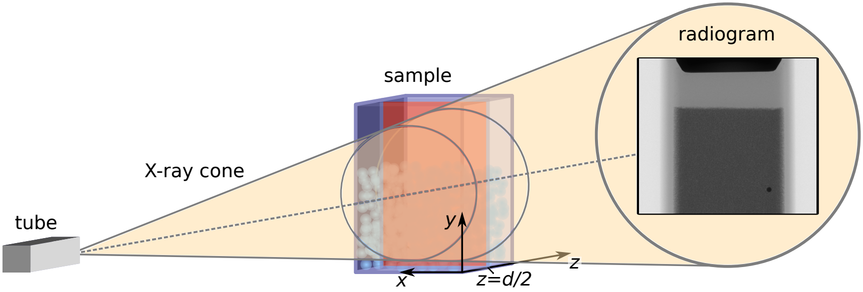

Tracking of particle front

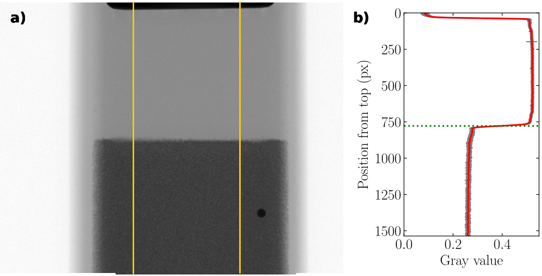

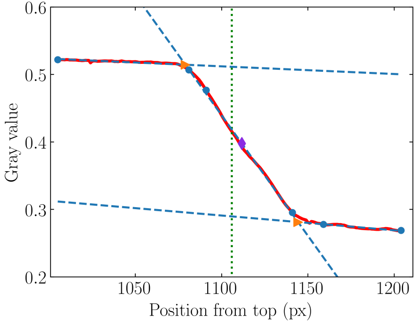

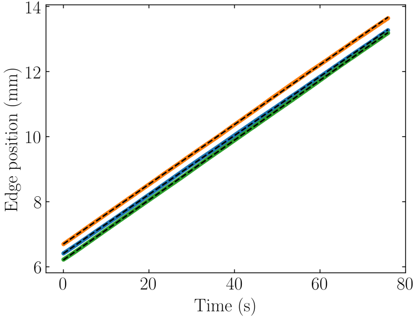

The image structure function $D(\mathbf{q}, \tau)$

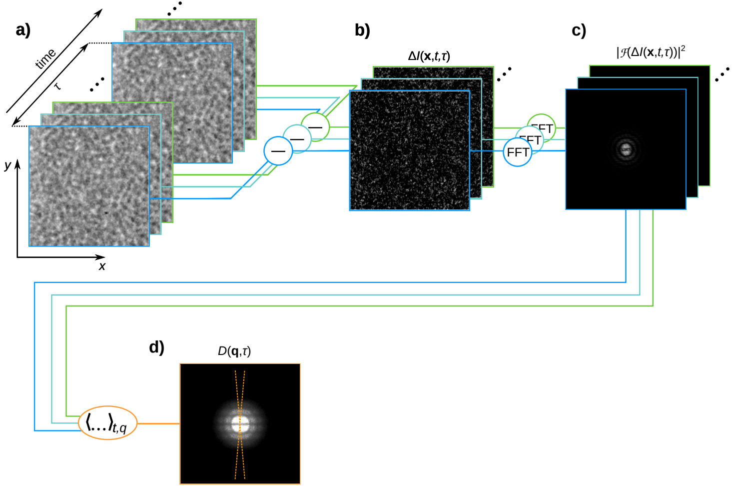

In collaboration with Manuel Escobedo, University of Düsseldorf

The image structure function $D(\mathbf{q}, \tau)$

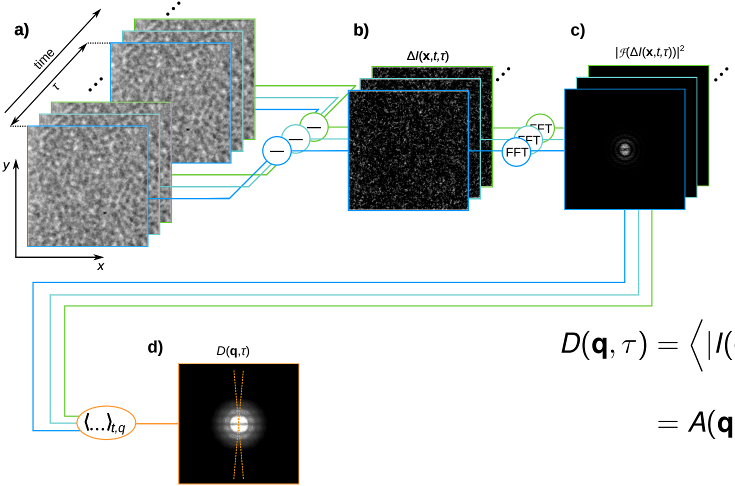

$$D(\mathbf{q}, \tau) = \left\langle |I(\mathbf{q}, t+\tau) - I(\mathbf{q}, t)|^2 \right\rangle_t$$

$$= A(\mathbf{q}) \left[1 - \frac{\langle I^*(\mathbf{q}, t) I(\mathbf{q}, t+\tau) \rangle_t}{\langle |I(\mathbf{q}, t)|^2 \rangle_t} \right] + B(\mathbf{q})$$

- $D(\mathbf{q}, \tau \to 0) = B(\mathbf{q})$
- $D(\mathbf{q}, \tau \to \infty) = A(\mathbf{q}) + B(\mathbf{q})$

In collaboration with Manuel Escobedo, University of Düsseldorf

The image structure function $D(\mathbf{q}, \tau)$

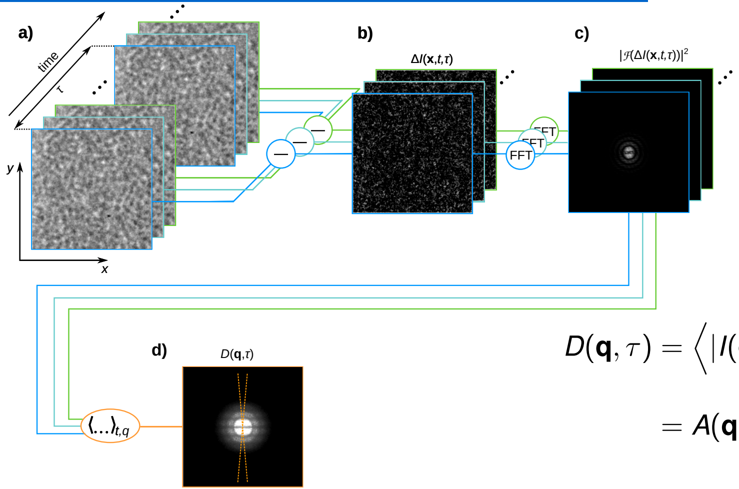

Linear space invariant imaging

$$f(\mathbf{q}, \tau) = \frac{\langle \rho^*(\mathbf{q}, t)\rho(\mathbf{q}, t+\tau)\rangle_t}{\langle |\rho(\mathbf{q}, t)|^2\rangle_t}$$

Intermediate scattering function

$$D(\mathbf{q}, \tau) = \left\langle |I(\mathbf{q}, t+\tau) - I(\mathbf{q}, t)|^2 \right\rangle_t$$

$$= A(\mathbf{q}) \left[1 - \frac{\left\langle I^*(\mathbf{q}, t) I(\mathbf{q}, t+\tau) \right\rangle_t}{\left\langle |I(\mathbf{q}, t)|^2 \right\rangle_t} \right] + B(\mathbf{q})$$

- $D(\mathbf{q}, \tau \to 0) = B(\mathbf{q})$
- $D(\mathbf{q}, \tau \to \infty) = A(\mathbf{q}) + B(\mathbf{q})$

In collaboration with Manuel Escobedo, University of Düsseldorf

X-ray imaging – Linear space invariant?

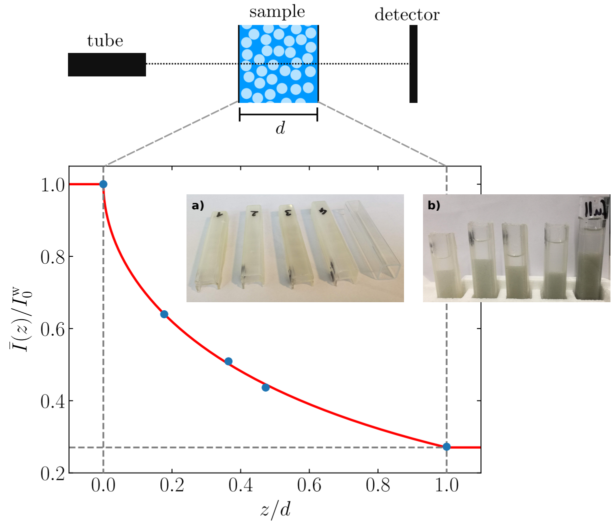

X-ray imaging – Linear space invariant?

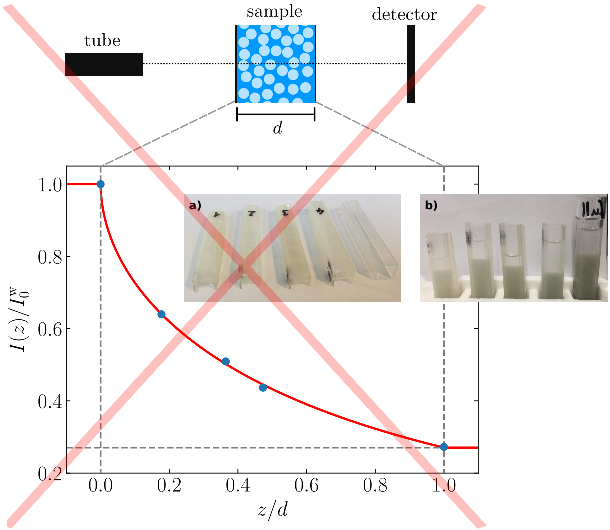

X-ray imaging – Linear space invariant?

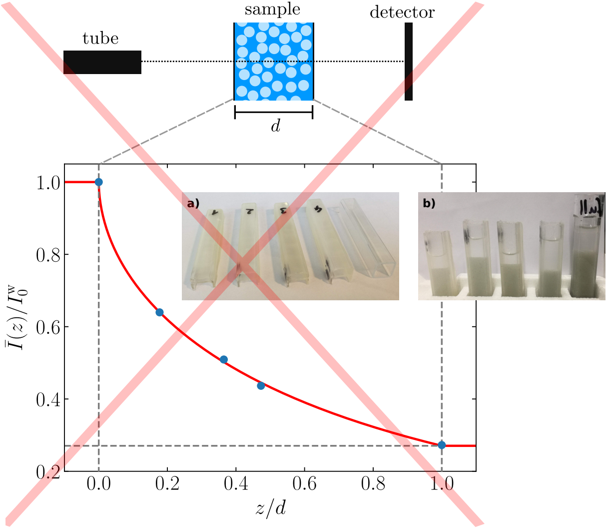

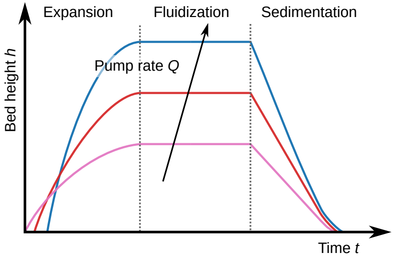

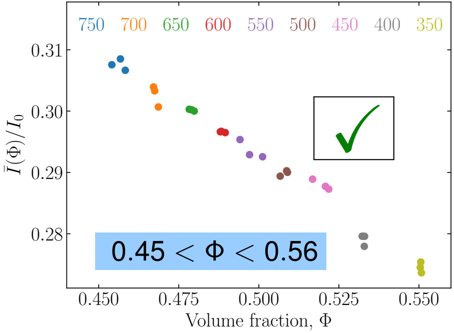

Estimate width of boundary layer

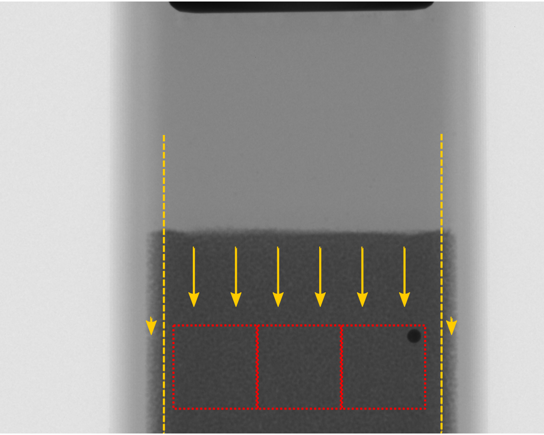

$\langle v \rangle_{\text{xdfa}} > \langle v \rangle_{\text{front}}$ by 9.4%

$\langle v \rangle_{\text{xdfa}}$ takes two layers into account

$\langle v \rangle_{\text{front}}$ takes four layers into account

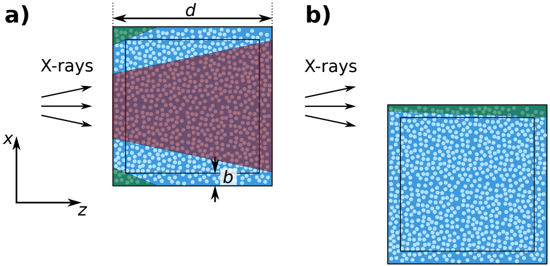

Estimation:

Boundary velocity = 0

Else = const.

$\rightarrow b \approx 3$ particle diameters